Localization and in-vivo characterization of thapsia garganica CYP76AE2 indicates a role in thapsigargin biosynthesis

Andersen, Trine Bundgaard; Martinez-Swatson, Karen Agatha; Rasmussen, Silas Anselm; Boughton, Berin Alain; Jørgensen, Kirsten; Andersen-Ranberg, Johan; Nyberg, Nils; Christensen, Søren Brøgger; Simonsen, Henrik Toft

Published in:
Plant Physiology

Link to article, DOI:
10.1104/pp.16.00055

Publication date:
2017

Document Version
Peer reviewed version

Localization and characterization of CYP76AE2 part of thapsigargin biosynthesis in Thapsia garganica

Andersen, Trine Bundgaard; Martinez-Swatson, Karen Agatha; Rasmussen, Silas Anselm; Boughton, Berin Alain ; Jørgensen, Kirsten; Andersen-Ranberg, Johan; Nyberg, Nils; Christensen, Søren Brøgger; Simonsen, Henrik Toft

Published in:
Plant Physiology

Link to article, DOI:
10.1104/pp.16.00055

Publication date:
2017

Document Version
Peer reviewed version

Plant Physiology Preview. Published on March 8, 2017, as DOI:10.1104/pp.16.00055

1 Localization of thapsigargin biosynthesis

2

3 Corresponding author(s):
4 Henrik Toft Simonsen
5 Department of Biotechnology and Biomedicine, Technical University of Denmark Søltofts Plads,
6 2800 Kgs. Lyngby, Denmark
7 +45 26986684
8 hets@dtu.dk

9

Localization and *in-vivo* characterization of *Thapsia garganica* CYP76AE2 indicates a role in thapsigargin biosynthesis

Trine Bundgaard Andersen, Karen Agatha Martinez-Swatson, Silas Anselm Rasmussen, Berin Alain Boughton, Kirsten Jørgensen, Johan Andersen-Ranberg[2], Nils Nyberg[3], Søren Brøgger Christensen, Henrik Toft Simonsen*

Department of Plant and Environmental Sciences, University of Copenhagen, Thorvaldsensvej 40, 1871 Frederiksberg C, Denmark (T.B.A, K.J, J.A-R.); Natural History Museum of Denmark, University of Copenhagen, Østervoldgade 5-7, DK-1350 Copenhagen K, Denmark (K.A.M.); Department of Biotechnology and Biomedicine, Technical University of Denmark, Søltofts Plads, 2800 Kgs. Lyngby, Denmark (K.A.M., S.A.R., H.T.S.); Metabolomics Australia, School of BioSciences, University of Melbourne, VIC, Australia, 3010 (B.A.B.); Department of Drug Design and Pharmacology, University of Copenhagen, Universitetsparken 2, 2100 Copenhagen, Denmark (N.N., S.B.C.)

One sentence Summary

The secretory ducts in the root of *Thapsia garganica* harbor the cytotoxin thapsigargin and the cells lining these ducts express the first enzymes in the biosynthesis of thapsigargin.

---

[1] This work was supported by SpotLight, a grant from the Danish Council for Strategic Research (T.B.A., H.T.S., S.B.C.). The work was supported by the Center for Synthetic Biology "bioSYNergy", UCPH Excellence Program for Interdisciplinary Research (J.A-R.) and by MEDPLANT, a Marie Curie Actions Initial Training Network (K.A.M.). NMR equipment used here was purchased via grant #10-085264 from The Danish Research Council for Independent Research | Nature and Universe.

[2] Present address: 441 Koshland Hall, Berkeley, CA 94720-3102, USA, joar@berkeley.edu

[3] Present address: Vallgatan 5, Bruker BioSpin Scandinavia AB, SE-170 67 Solna, Sweden

* Address correspondence to hets@dtu.dk

The author responsible for distribution of materials integral to the findings presented in this article in accordance with the policy described in the Instructions for Authors (www.plantphysiol.org) is: Henrik Toft Simonsen (hets@dtu.dk).

T.B.A. established the major part of the results and prepared the major part of the paper. K.A.M. prepared samples for MALD, performed the *in situ* PCR experiment and contributed to the manuscript. S.A.R. purified epidihydrocostunolide. S.B.C., S.A.R. and N.N. performed the NMR. B.A.B. performed the MALDI analysis. J.A.R. did part of the purification of compound **2** and **3**, K.J. contributed to the *in situ* PCR experiment. H.T.S. initiated, directed and supported the research and writing of the manuscript. All authors edited and approved the final manuscript.

Abstract

The Mediterranean plant *Thapsia garganica* (dicot, Apiaceae), also known as Deadly carrot, produces the highly toxic compound thapsigargin. This compound is a potent inhibitor of the SERCA calcium pump in mammals, and is of industrial importance as the active moiety of the anticancer drug Mipsagargin, currently in clinical trials. Knowledge of thapsigargin *in planta* storage and biosynthesis has so far been limited. Here we present the putative second step in thapsigargin biosynthesis, by showing that the cytochrome P450 *Tg*CYP76AE2, transiently expressed in *Nicotiana benthamiana*, converts epikunzeaol into epidihydrocostunolide. Furthermore, we show that thapsigargin is likely to be stored in secretory ducts in the roots. Transcripts from *Tg*TPS2 (epikunzeaol synthase) and *Tg*CYP76AE2 in roots were only found in the epithelial cells lining these secretory ducts. This emphasizes the involvement of these cells in the biosynthesis of thapsigargin. This study paves the way for the further studies of thapsigargin biosynthesis.

Introduction

Sesquiterpenoids are widely distributed across the plant kingdom and are recognized for their pharmacological properties and commercial value (Simonsen et al., 2013). Artemisinin, which today is the cornerstone for treatment of malaria, is an outstanding example (Wiesner et al., 2003; Tu, 2011), along with fragrances such as patchoulol and santalol (Zhan et al., 2014). The genus *Thapsia* L. (Apiaceae) produces a variety of sesquiterpenoids including sesquiterpene lactones (Christensen et al., 1997; Drew et al., 2009). The most studied sesquiterpene from the genus is the sesquiterpene lactone thapsigargin, which is the most predominant sesquiterpene lactone in *Thapsia garganica* L. and *Thapsia gymnesica* Rouy (Christensen et al., 1997). In the Mediterranean area *T. garganica* has been used in traditional medicine for over 2000 years for the treatment of pulmonary diseases, catarrh, fever, pneumonia and as a counter irritant for the relief of rheumatic pains (Andersen et al., 2015). The pharmacological effect of thapsigargin has been studied thoroughly and it has been established that thapsigargin is an inhibitor of the sarco-endoplasmic reticulum Ca^{2+}-ATPase (SERCA) that leads to cell apoptosis (Thastrup et al., 1990). A pro-drug (Mipsagargin®) based on thapsigargin towards solid cancer tumors is currently in clinical trials (Doan et al., 2015; Mahalingam et al., 2016).

An unusual feature of thapsigargin and related guaianolides is the presence of a β-disposed C-6-O and an α-disposed C-7-C-11 bond. In the majority of guaianolides from other plant families, the C-6-O bond is α-disposed and the C-7-C-11 bond β-disposed (Christensen et al., 1997; Drew et al., 2009; Simonsen et al., 2013).

Thapsigargin is found in most parts of the plant *T. garganica*. Ripe fruits contain the highest amount of thapsigargin with 0.7-1.5% of the dry weight followed by roots (0.2-1.2% d.w.) and leaves (0.1% d.w.) (Smitt et al., 1995). It is well established that many Apiaceae species store lipophilic compounds such as phenyl propanoids and terpenoids in secretory ducts and vittae (Corsi et al., 1988; Poli et al., 1995; Maggi et al., 2015). We chose to examine the localization of sesquiterpenoids and their biosynthesis in *T. garganica* roots that have high amounts of thapsigargin. The roots could also be obtained commercially from plants grown in greenhouses, in contrast to the seasonal dependent harvest of fruits from the natural population. Fruits have so far not been obtained from greenhouse plants, not even from plants more than four years old. By histochemical staining, we show that *T. garganica* roots contain secretory ducts in parenchymatic tissue and that these may harbor terpenoids. Matrix-Assisted Laser Desorption Ionization Mass Spectrometry Imaging (MALDI-MSI) of the roots was used to show that thapsigargin is present in

specific locations in the root and furthermore in a pattern likely to coincide with the location of secretory ducts.

The site and route of thapsigargin biosynthesis have not yet been established. The first specific step in the biosynthesis of most sesquiterpenoids is catalyzed by sesquiterpene synthases (Bohlmann et al., 1998). Two sesquiterpene synthases have previously been described from *T. garganica* roots. These were expressed in *Saccharomyces cerevisiae* and biochemically characterized. It was shown that the sesquiterpenoid synthase *Tg*TPS2 was of particular interest to thapsigargin biosynthesis. The major product of *Tg*TPS2 is epikunzeaol, a germacrenol with a hydroxyl group at C-6 (Figure 1) (Pickel et al., 2012).

Generally, the diversity of sesquiterpenoids is obtained by the catalytic activity of the sesquiterpene synthases and followed by modifications to the C_{15} backbone by cytochromes P450 (P450s), acyl transferases and dehydrogenase amongst others (Weitzel and Simonsen, 2015). Complexity of sesquiterpenoid structures, including chiral centers and regio- and stereospecific oxidations, makes chemical synthesis difficult and synthesis approaches often result in low yields (Andrews et al., 2007; Ball et al., 2007; Chu et al., 2016). Attempts to find alternative sustainable production methods for sesquiterpenoids such as artemisinin by biological synthesis are actively pursued (Paddon et al., 2013). Sesquiterpenoid lactones are a subgroup of sesquiterpenoids, and compounds in this subgroup have been shown to have a potential for treatment of various cancers (Curry et al., 2004; Simonsen et al., 2013). Despite recent advances, only a few steps in the complex biosynthetic routes of plant sesquiterpenoid lactones have been characterized. These include enzymes involved in the biosynthesis of artemisinin (*Artemisia annua* L.) and (+)-costunolide, a precursor for a range of other sesquiterpene lactones (in *Cichorium intybus* L. and *Tanacetum parthenium* L.). These plants are all from the family Asteraceae (Yu and Wen, 2011; Liu et al., 2014).

P450s are common participators in sesquiterpenoid biosynthesis and especially P450s from the CYP71 clan have been shown to be involved in the biosynthesis of sesquiterpenoids (Luo et al., 2001; Diaz-Chavez et al., 2013; Liu et al., 2014; Takase et al., 2015; Weitzel and Simonsen, 2015; Yang et al., 2015). CYP71AV1, which is involved in artemisinin biosynthesis, is among the most well studied P450s in sesquiterpenoid biosynthesis (Teoh et al., 2006). Here we functionally characterize *Tg*CYP76AE2, a P450 from the CYP71 clan, which was found in the root transcriptome of *T. garganica*. Through the transient co-expression in *Nicotiana benthamiana* of *Tg*TPS2 and *Tg*CYP76AE2, epikunzeaol is converted to epidihydrocostunolide, a likely precursor for more complex sesquiterpenoid lactones including thapsigargin. Within the Apiaceae, only P450s

involved in the biosynthesis of the phenylpropanoid coumarin have been described (Larbat et al., 2007; Larbat et al., 2009; Drew et al., 2013; Dueholm et al., 2015). This work presents the

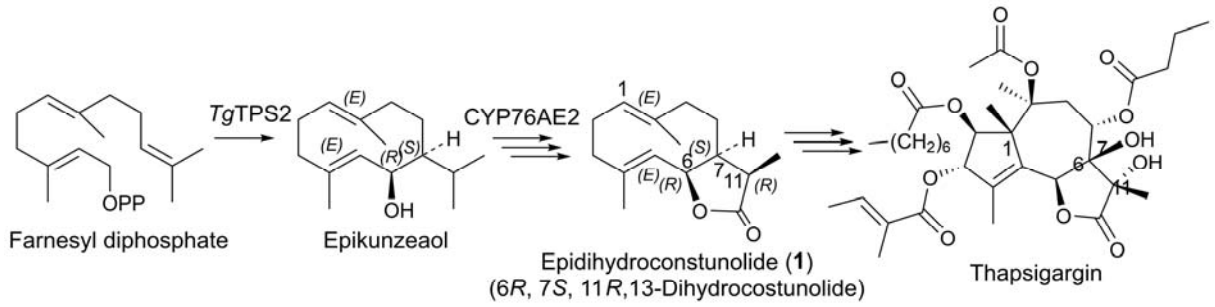

Figure 1. The structure of epikunzeaol and epidihydrocostunolide (**1**). Both metabolites are suggested intermediates in the thapsigargin pathway in *T. garganica*.

functional characterization of the first sesquiterpene specific P450 found in the Apiaceae. *In situ* PCR was performed to investigate the specific site for expression of *Tg*TPS2 and *Tg*CYP76AE2. We were thereby able to verify that *Tg*TPS2 and *Tg*CYP76AE2 are expressed in epithelial cells lining the secretory ducts containing thapsigargin.

Results

Identification of cytochromes P450 from transcriptome data

The root transcriptome data from *T. garganica* were mined to enable the discovery of possible sequential biosynthesis steps from epikunzeaol toward thapsigargin. The search was limited to P450s from the CYP71 clan due to the previous findings in this clan of P450s involved in sesquiterpenoid biosynthesis. We investigated the occurrence of orthologous genes to CYP71's in the *T. garganica* transcriptome using BLAST searches. The eighteen full-length P450 genes were found to be distributed with twelve belonging to the CYP71 family, one to the CYP706 family and five to the CYP76 family. The P450s were named by David Nelson according to the current annotation system (Nelson, 2009); *TgCYP71AH8* (KX826939), *TgCYP71AJ5* (KP191555), *TgCYP71AJ14* (KP191558), *TgCYP71AS14* (KX845553), *TgCYP71AT12* (KX826940), *TgCYP71AU89* (KX845548), *TgCYP71AU90* (KX845552), *TgCYP71BK1* (KX826941), *TgCYP71BK6* (KX845546), *TgCYP71D183* (KX845554), *TgCYP71D311* (KX845555), *TgCYP71D319_ortholog* (KX845550), *TgCYP76AE1* (KX826942), *TgCYP76AE2* (KX826943), *TgCYP76AE8* (KX845545), *TgCYP76AF7* (KX845549), *TgCYP76B79* (KX845547) and *TgCYP706C30_ortholog* (KX845551)

Phylogeny

Phylogenetic analyses of 35 full-length genes from the CYP71 clade involved in sesquiterpenoid biosynthesis from several plant species and the 18 enzymes from *T. garganica* revealed that these enzymes are grouped in several subclades (Figure 2). The analysis shows that there are blooms of genes within species and families (Hamberger and Bak, 2013), like the CYP76F bloom in *Santalum album*. Allthough, the phylogeny only included P450s related to sesquiterpenoid metabolism, the seqeunces are from most families and subfamilies in the CYP71 clade. This shows that phylogenetic analysis are not a useful to predict specific functionality of P450s, as also shown previously (Dueholm et al., 2015). The analysis merely serve to indicate what range of enzymes that have to be examined biochemically; in this case 18 sequences.

.

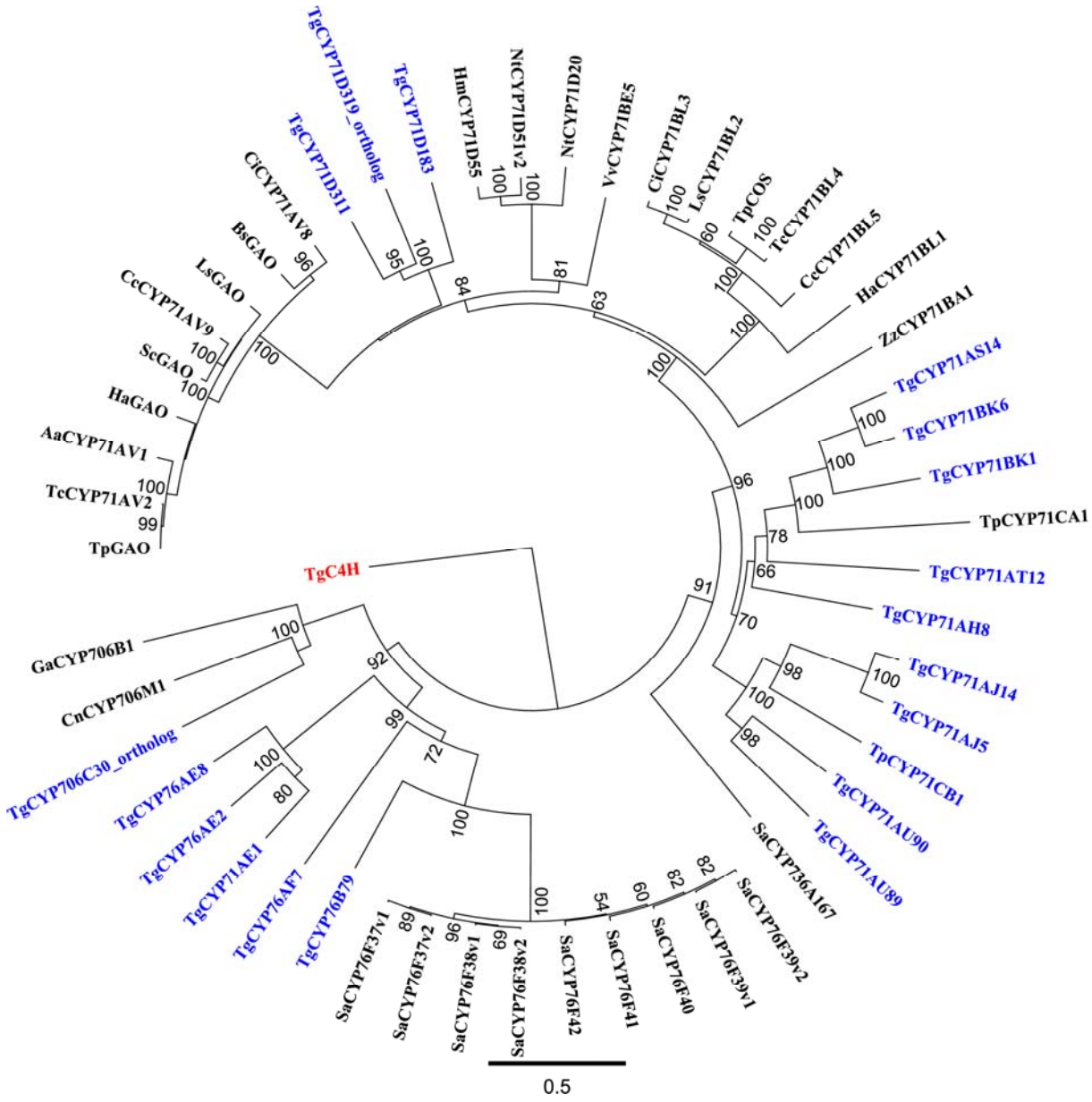

GC-MS and LC-MS analysis of extracts from *N. benthamiana* expressing *Tg*TPS2 and cytochromes P450, including *Tg*CYP76AE2

The cyclodeca-1(10),4-diene ring of epikunzeaol (Figure 1) is susceptible to thermal Cope rearrangement at the high temperatures in the GC-MS injection port. Extracts of *N. benthamiana* expressing *At*HMGR and *Tg*TPS2 were therefore analyzed with the two injection port temperatures, 250°C and 160°C. At 250°C, the *Tg*TPS2 product epikunzeaol is detected along with degradation compounds whereas at 160°C, only epikunzeaol is detected (Figure 3A). Similar rearrangement have been identified for other cyclodeca-1(10),4-diene products of sesquiterpene synthases (Andersen et al., 2015). To enhance the level of precursors available for *Tg*TPS2 in *N.*

benthamiana, a truncated version of the *Arabidopsis thaliana* HMGR, *At*tHMGR, was transiently co-expressed. *At*tHMGR has previously been shown to enhance production levels of sesquiterpenoids (Cankar et al., 2015).

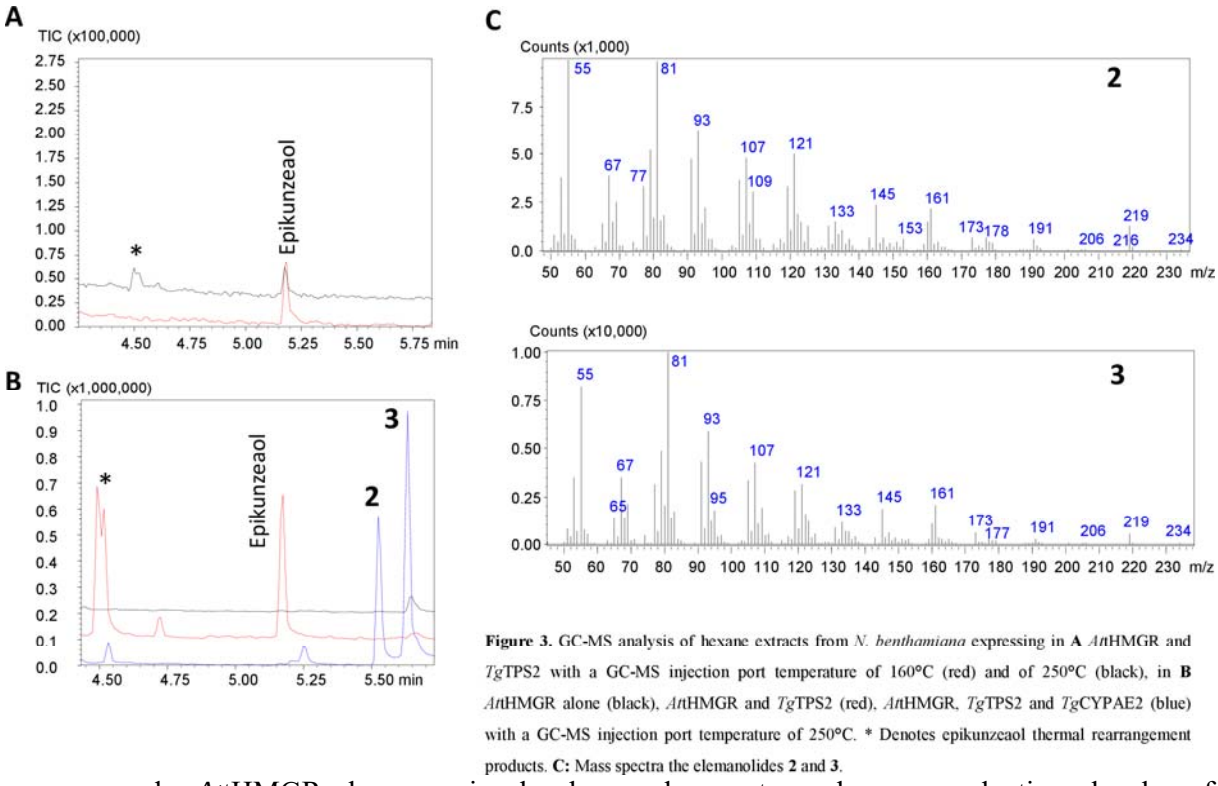

Figure 3. GC-MS analysis of hexane extracts from *N. benthamiana* expressing in **A** *At*tHMGR and *Tg*TPS2 with a GC-MS injection port temperature of 160°C (red) and of 250°C (black), in **B** *At*tHMGR alone (black), *At*tHMGR and *Tg*TPS2 (red), *At*tHMGR, *Tg*TPS2 and *Tg*CYPAE2 (blue) with a GC-MS injection port temperature of 250°C. * Denotes epikunzeaol thermal rearrangement products. **C:** Mass spectra the elemanolides **2** and **3**.

In order to discover, which P450(s) that could utilize epikunzeaol as substrate the eighteen P450s from the CYP71 clan were transiently co-expressed with *Tg*TPS2 and *At*tHMGR in *N. benthamiana*.

Of the tested P450s, only *Tg*CYP76AE2 was evidently able to utilize epikunzeaol as a substrate. To test for further downstream pathway steps the remaining P450s were co-expressed with *At*tHMGR, *Tg*TPS2 and *Tg*CYP76AE2. No new products or decline in substrate was detected. At this stage, it cannot be excluded that new products were not detected due to low expression or lack of expression of the seventeen P450s.

GC-MS analysis of the hexane extracts of *N. benthamiana* leaves expressing *At*tHMGR, *Tg*TPS2 and *Tg*CYP76AE2 is shown in Figure 3B, where two new products, **2** and **3**, are observed. It was not possible to detect these products with the injection port at 160°C, which can be explained by a lower volatility of the new product(s) in comparison with epikunzeaol. The co-expression of *At*tHMGR, *Tg*TPS2 and *Tg*CYP76AE2 in *N. benthamiana* resulted in a complete conversion of epikunzeaol (Figure 3B).

To expand the search for *Tg*CYP76AE2 products or derivatives hereof, not detectable by GC-MS, the *N. benthamiana* extracts was analyzed by analytical LC-MS. In contrast to the GC-MS analysis, epikunzeaol was not detected in free form, but as the aglycon in a glycoside of a disaccharide , and only one *Tg*CYP76AE2 product was detected (Figure 4). In the LC-MS analysis product **1** was detected as the protonated molecular ion (*m/z* 235.23, $[M+H]^+$), the sodium adduct (*m/z* 257.23, $[M+Na]^+$), and the base peak equal to *m/z* 491.3126 ($[2M+Na]^+$), corresponding to the sodiated dimer adduct.

Isolation of epidihydrocostunolide (1) and the two 1,3-elemandien-12,6-olides (2 and 3) by HPLC and preparative GC-MS for NMR analysis.

To determine the structure of the three new compounds (**1**, **2**, and **3**) these were isolated from the hexane extract of *N. benthamiana* leaves expressing *At*tHMGR, *Tg*TPS2 and *Tg*CYP76AE2. Compound **1** was isolated by semi-preparative normal-phase HPLC and the purity was confirmed by LC-HRMS. Compounds **2** and **3** were isolated using preparative GC-MS. To confirm that **2** and **3** are thermal Cope rearrangement products of **1**, pure **1** was injected into the GC-MS (Figure 5). No traces of compound **1** was seen in this GC-MS chromatogram, whereas the mass spectra of the peaks originating in compound **2** and **3** were identical to those obtained from the compounds isolated by preparative GC-MS (Figure S2). This confirm the thermal Cope rearrangement of **1** into **2** and **3**.

Structure elucidation of product 1, 2 and 3

The structures of **1**, **2** and **3** were elucidated by the interpretation of ^{1}H, ^{13}C and 2D COSY, HSQC, HMBC and ROESY spectra. The molecular formula of **1** was established using High Resolution Mass Spectrometry (HRMS) to be $C_{15}H_{22}O_2$ (observed *m/z* 235.1692, calculated for $C_{15}H_{22}O_2$ $[M+H]^+$ *m/z* 235.1693, 0.2 ppm error). Comparison of the ^{1}H and ^{13}C NMR spectra of **1** with that of dihydrocostunolide and in particular the ^{13}C NMR spectrum (Sanz et al., 1990; Barrero et al., 2002) revealed significant similarities. The structure elucidation was complicated as all nuclei exhibited one major signal and a minor signal, as is clearly observed in the ^{13}C NMR spectrum (Figure S1). This is most likely an effect caused by the presence of two slowly interconverting conformers of the decadiene ring. However, closer inspection showed that the isolated germacranolide had to be a stereoisomer of the previously proposed structure of dihydrocostunolide. The ROE interactions between H-7, H-11 and H-6 indicated that these protons were all cis-disposed, thus supporting the proposed structure of **1**.

From the preparative GC-MS isolation, two products (**2** and **3**) were obtained (Figure 3B). Compound **2** had the molecular formula $C_{15}H_{22}O_2$ as revealed by MS. Inspection of the ^{13}C NMR spectrum indicated the presence of two signals for methylene groups at 110 and 116, a signal for a quaternary carbon at 144 (Table 1). A signal for a methine group at 149 ppm suggested the presence of a mono substituted and a germinal di-substituted double bond, respectively. A signal for a carbonyl group at 179 ppm indicated the presence of a γ-lactone. These chemical shift values were

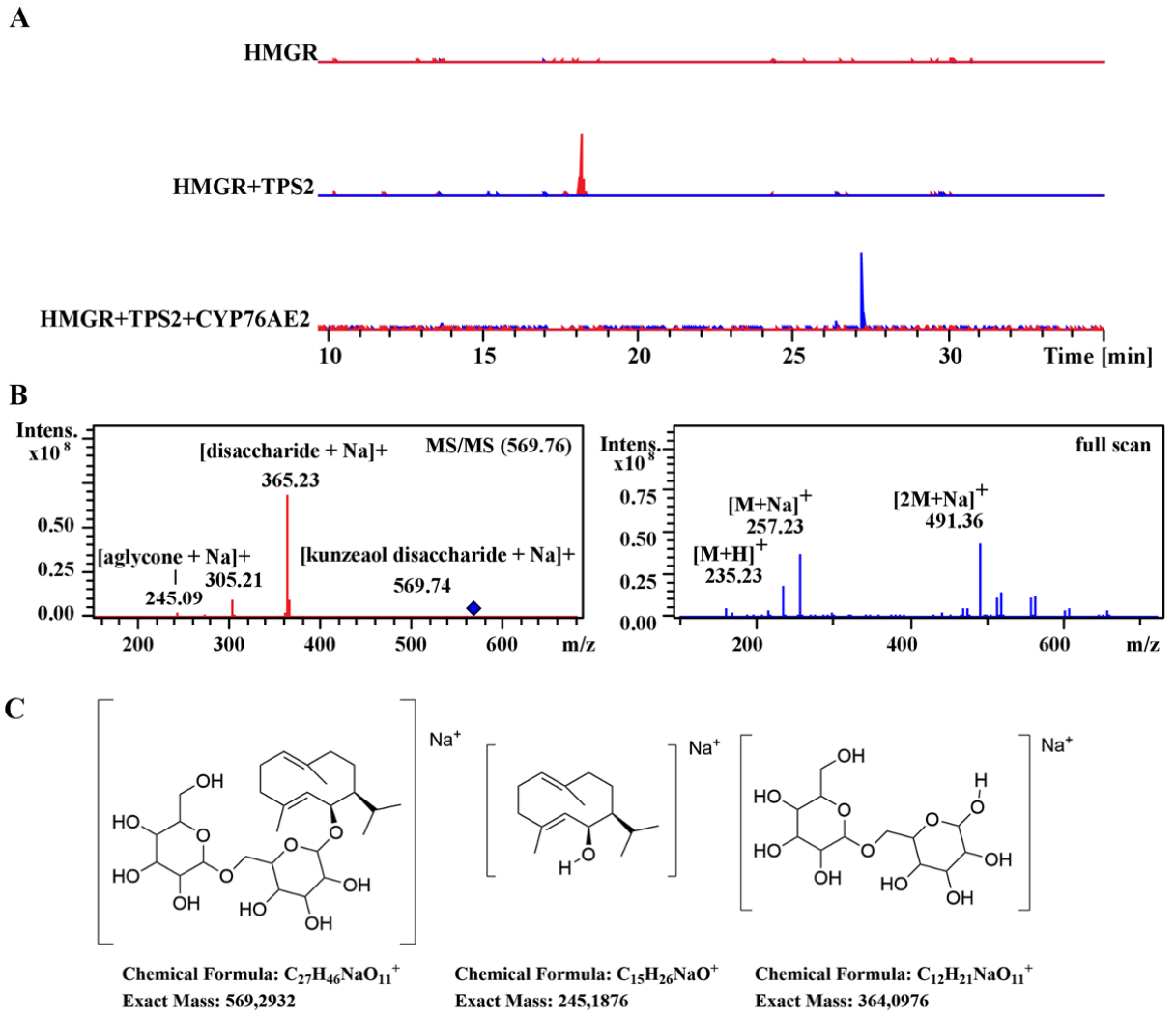

Figure 4: **A**:Extracted Ion Chromatograms of epikunzeaol [epikunzeaol disaccharide+Na]+ *m/z* 569.74 (red) and epidihydrocostunolide [2M+Na]+ *m/z* 491.32 (blue) of the LC-MS analysis of methanol extract of *At*tHMGR alone, *At*tHMGR plus *Tg*TPS2, and *At*tHMGR plus *Tg*TPS2 and *Sl*CYP76AE2.
B: The MS/MS spectrum of the epikunzeaol peak at 18 minutes detected as the epikunzeaol disaccharide. The MS spectrum of epidihydrocostunolide at 27 minutes shows a *m/z* of 491.3258corresponding to a sodium adduct and a dimer of *m/z* 235.1741.
C: The structure of epikunzeaol disaccharide including the fragmentation pattern.

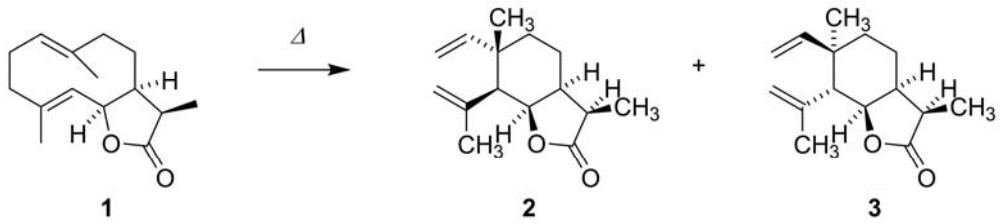

Figure 5: Thermal rearrangement of **1** into the two compounds **2** and **3**. The Cope rearrangement is well known for transforming germacradi-1(10),4-dienolides into elemanolides.

very similar to those reported for the saussurea lactone (Barrero et al., 2002). Inspection of the ^{1}H NMR spectrum of **2** (Table 2) and the reported spectrum of the saussurea lactone (Ando et al., 1983) however, revealed significant differences between the sizes of the 3-bond coupling constants in **2** and in the saussurea lactone. In the saussurea lactone, the lactone ring is *trans*-fused with the cyclohexane ring, enabling an axial location of H-6 and H-7 and consequently coupling constants of approximately 10 Hz are expected. Assuming that the lactone ring and the cyclohexane ring of **2** are *cis*-fused this would prevent an axial-axial coupling and consequently smaller $^{3}J_{HH}$ couplings are expected. Inspection of the ROESY spectrum also revealed ROE-correlation between H-6 and H-7 confirming the *cis*-fusion. An additional ROE-correlation between H-7 and H-11 revealed that these protons also are *cis*-disposed. ROE-correlations between CH_3-15, CH_3-14 and CH_3-13 confirm that all of these methyl groups are β-disposed. Based on the data the stereochemistry of **2** is suggested as shown in Figure 5 to be (3*R*,3a*S*,6*S*,7*S*,7a*R*)-3,6-dimethyl-7-(prop-1-en-2-yl)-6-vinylhexahydrobenzofuran-2(3H)-one.

The spectra of **3** were very similar to those of **2**. In **3** however, a similar ROE-correlation as described above for compound **1** was present except for ROE-correlation between CH_3-15 and CH_3-13. Combined with similar $^{3}J_{HH}$ coupling constants this suggest the stereochemistry of **3** shown in Figure 5 to be (3*R*,3a*S*,6*R*,7*R*,7a*R*)-3,6-dimethyl-7-(prop-1-en-2-yl)-6-vinylhexahydrobenzofuran-2(3H)-one. **1** is a new compound for which, we suggest the name epidihydrocostunolide. The stable structure of **2** and **3** led to the full structure elucidation of **1**.

Tissue localization of thapsigargin biosynthesis in roots

Histochemical staining and MALDI-MS imaging (MALDI-MSI) was performed to determine the localization of thapsigargin and its biosynthesis. Histochemical staining was used to indicate the presence of terpenoids in secretory ducts in root tissue. The location of thapsigargin was analyzed by MALDI-MSI. Based on these results further investigations by *in situ* PCR was performed to observe if the expression of *Tg*TPS2 and *Tg*CYP76AE2 involved in the biosynthesis of thapsigargin showed co-localization with thapsigargin.

230 **Histochemical analysis of *T. garganica* roots**

231 The presence of special storage structures in the root possibly containing terpenoids was
232 investigated by a histochemical analysis using NADI staining (David and Carde, 1964; Caissard et
233 al., 2004; Jezler et al., 2013; Kromer et al., 2016; Muravnik et al., 2016; Stešević et al., 2016;
234 Stojičić et al., 2016). The NADI reagent has been reported to give rise to a blue/purple color in the
235 presence of oxygenated or lipophilic compounds (e.g. terpenoids) in oil secretory cells such as
236 ducts, trichomes and other specialized tissue. NADI is a two component system consisting of
237 dimethyl-p-phenylenediamine and α–naphathol. The mechanism is suggested to be a non-enzymatic
238 reduction of the oxidized target and an oxidation of dimethyl-p-phenylenediamine followed by the
239 formation of a radical, which react with α–naphathol to produce indophenol blue (Harwig, 1967;
240 Takamatsu and Hirai, 1968).

241 Prior to staining, *T. garganica* roots were cut in 60 µm cross-sections. As in other *Daucus* species
242 the roots showed a clear secondary growth (Havis, 1939; Korolev et al., 2000). White resin was
243 observed oozing out of the root upon cutting. Figure 6 indicates the presence of oxygenated or
244 lipophilic compounds (e.g. terpenoids) in the sections after staining with NADI and here secretory
245 ducts are clearly visible as blue spots. These were located in concentric rings within the
246 parenchymatic tissue radiating out from the pith until just below the periderm as also shown in
247 *Daucus* (Deutschmann, 1969). At higher magnification, it is evident that both the ducts themselves
248 and the epithelial cells surrounding these were stained blue indicating the presence of oxygenated or
249 lipophilic compounds (e.g. terpenoids). Apart from the ducts in the parenchymatic tissue the
250 periderm also showed blue staining, which could be due to tannins in this tissue. In general, ducts
251 were not found in cross-sections from the crown or the very bottom of the roots, but otherwise
252 generally distributed throughout the root.

253 **MALDI-MSI of *T. garganica* roots**

254 The spatial distribution of thapsigargin, the intermediates epikunzeaol and epihydrocostunolide;
255 including related guaianolides were examined using High Resolution Matrix Assisted Laser
256 Desorption Ionization-Fourier Transform-Ion Cyclotron Resonance-Mass Spectrometry Imaging
257 (HR MALDI-FT-ICR-MSI). MALDI-MSI is able to measure ionized chemicals as their mass-to-
258 charge ratio (*m/z*) in a highly localized manner (Boughton et al., 2016). Root sections of *T.*
259 *garganica*, that had previously been confirmed to contain thapsigargin by HPLC, were prepared by
260 initial cryo-sectioning, mounting to slides on double sided tape, freeze drying and application of
261 DHB matrix by sublimation (Jarvis et al., 2017). Prepared sections were analyzed by MALDI-MSI

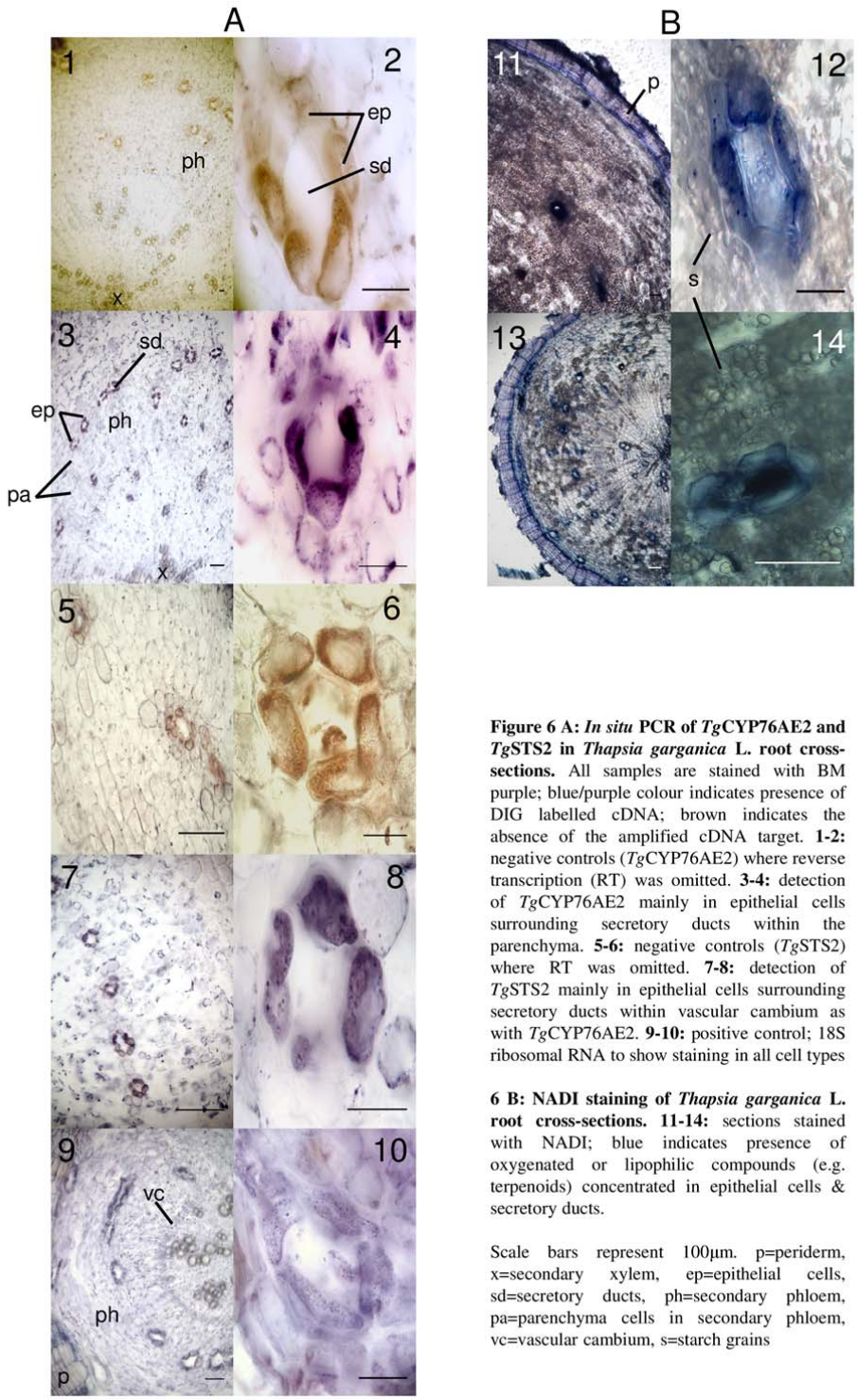

Figure 6 A: *In situ* PCR of *Tg*CYP76AE2 and *Tg*STS2 in *Thapsia garganica* L. root cross-sections. All samples are stained with BM purple; blue/purple colour indicates presence of DIG labelled cDNA; brown indicates the absence of the amplified cDNA target. **1-2:** negative controls (*Tg*CYP76AE2) where reverse transcription (RT) was omitted. **3-4:** detection of *Tg*CYP76AE2 mainly in epithelial cells surrounding secretory ducts within the parenchyma. **5-6:** negative controls (*Tg*STS2) where RT was omitted. **7-8:** detection of *Tg*STS2 mainly in epithelial cells surrounding secretory ducts within vascular cambium as with *Tg*CYP76AE2. **9-10:** positive control; 18S ribosomal RNA to show staining in all cell types

6 B: NADI staining of *Thapsia garganica* L. root cross-sections. 11-14: sections stained with NADI; blue indicates presence of oxygenated or lipophilic compounds (e.g. terpenoids) concentrated in epithelial cells & secretory ducts.

Scale bars represent 100µm. p=periderm, x=secondary xylem, ep=epithelial cells, sd=secretory ducts, ph=secondary phloem, pa=parenchyma cells in secondary phloem, vc=vascular cambium, s=starch grains

in the positive ionization mode across the mass range m/z 200-3000. Results demonstrated complex mass spectra containing numerous ions that could be tentatively assigned as small molecule metabolites, sugars and lipids (Figure S3). Specific ions were found to localize to the epidermis,

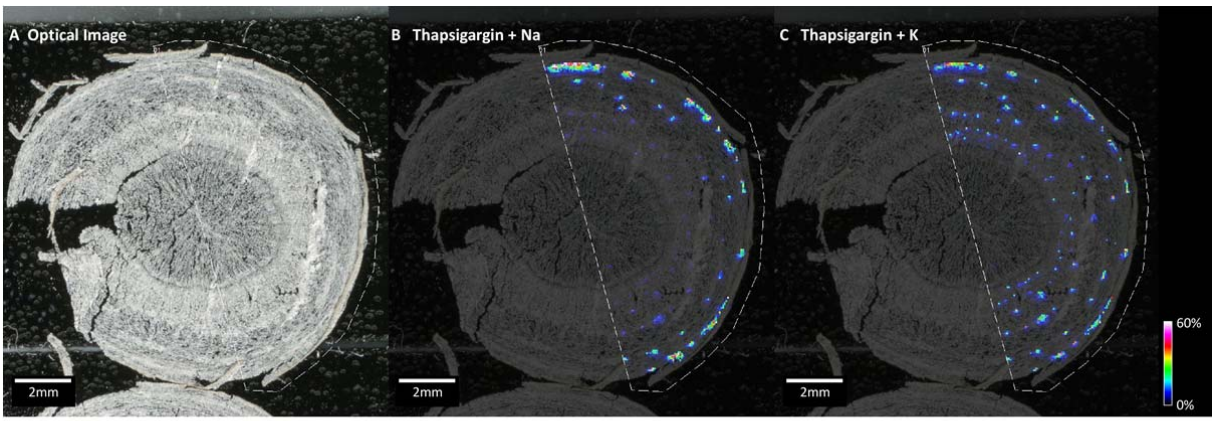

Figure 7. MALDI-MSI analysis of *T. garganica* taproot section. **A:** optical image of taproot section with sublimed DHB matrix, **B:** distribution of thapsigargin Na adduct, $[M+Na]^+$ *m/z* 673.3186 (calc. 673.31945, 1.26 ppm error), **C:** distribution of thapsigargin K adduct, $[M+K]^+$ *m/z* 689.2924 (calc. 689. 29339, 1.43 ppm error). Images normalized to RMS and scaled to 0-60 % of maximum signal intensity using FlexImaging 4.1 to enhance visualization. Results demonstrate thapsigargin to be localized to concentric circles of secretory ducts.

parenchyma, stele and a series of concentric spots correlating with the observed distribution of secretory ducts (Figure 7). The acquired spectra were screened for thapsigargin, epikunzeaol and epidihydrocostunolide by searching for the calculated *m/z* of proton, sodium and potassium adducts. Ions corresponding to thapsigargin, $[M+Na]^+$ ion *m/z* 673.3186 (calc. 673.31945, 1.26 ppm error) and a $[M+K]^+$ ion *m/z* 689.2924 (calc. 689.29339, 1.43 ppm error) were found. Proton adducts of thapsigargin were barely observed and in general the K adduct showed a much higher signal intensity relative to the Na adduct (signal intensity ratio of 2.5-3:1). The spatial distribution of both Na and K adducts showed a distinct distribution within the parenchymatic tissue (Figure 7), where the distribution pattern correlated with concentric circles of secretory ducts visualized from histochemical staining (Figure 6). Both epikunzeaol and epidihydrocostunolide were not detected in the images, indicating that concentrations were below the limit of detection using this methodology. The root sections were also screened for seven related guaianolides from *T. garganica* (Table 3). Structures of the related guanolides and the MALDI imaging results from these are shown in Figure S4. The seven structurally similar sesquiterpenoids, thapsigargicin, nortrilobolide, trilobolide, thapsivillosin I and thapsivillosin L all showed distributions that coincided with thapsigargin, including a similar pattern of a more intense $[M+K]^+$ adduct.

Localization of mRNA for *Tg*TPS2 and *Tg*CYP76AE2

Following the specific localization of thapsigargin in the roots and likely in secretory ducts it was investigated if the production of the compound takes place here as well. Cellular localization of transcripts encoding *Tg*TPS2 and *Tg*CYP76AE2, involved in the biosynthesis, was investigated by in tube *in situ* PCR. *Tg*TPS2 and *Tg*CYP76AE2 transcripts were found to show the same spatial expression pattern in the investigated tissue and were detected solely in the epithelial cells lining the

secretory ducts (Figure 6A and 6B). The presence of the transcripts were visualized by the color reaction of the alkaline phosphates bound to the antibody specific to the DIG group incorporated during the amplification of the PCR product from the specific produced cDNA using the reverse specific primers recognizing *Tg*TPS2 and *Tg*CYP76AE2 respectively. In *T. garganica* roots this reaction only took place in the epithelial cells of the secretory ducts when specific reverse primers where included. When no specific reverse primers were used no color reaction were detected. This reaction clearly shows that the ducts follow the circular growth pattern of the parenchymatic tissue. The transcripts show a spatial distribution similar to the *m/z* corresponding to thapsigargin as is seen in Figure 7.

Discussion

In this study, *Tg*CYP76AE2 was found to catalyze the oxidations that lead to the formation of a lactone ring hereby converting epikunzeaol into epidihydrocostunolide (**1**) (Figure 1). The structure of **2** and **3** confirm the proposed structure of **1** and also finally confirm the structure of epikunzeaol produced by *Tg*TPS2 as seen in Figure 1. The structure of kunzeaol previously published as the product of *Tg*TPS2 did not benefit from the Cope rearrangement study included here and the stereochemistry was therefore not final (Pickel et al., 2012). In general, Cope rearrangements are stereoselective and only one product would be expected (Setzer, 2008; Adio, 2009). However, here upon injection of **1** into a GC-MS two elemanolides, **2** and **3**, were formed in almost equal amounts (Figure S2). This type of rearrangement has been studied for sesquiterpenoids belonging to the germacrenes and germacranolides. Germacrenes are characteristic by their backbone structure, which is a 10-membered open ring as seen in epikunzeaol (Figure 1). Conversion of germacranolides to elemanolides by Cope rearrangement has previously been used to structurally elucidate the heat labile germacranolides (Fischer and Mabry, 1967; Takeda, 1974; Raucher et al., 1986; de Kraker et al., 2001; Barrero et al., 2002; Adio, 2009). At high temperatures or low pH germacrenes via Cope rearrangement establish equilibrium with elemenes (Takeda, 1974; de Kraker et al., 2002; Pickel et al., 2012). Elemenes are characteristic by the lack of a bond between C2 and C3 (Figure 4). The unexpected formation of two products after Cope-rearrangement of **1** might be explained by the *cis*-fused lactone and instability of the 10-membered decadiene ring. Most reported studies on Cope rearrangements have been performed on *trans*-fused germacranolides, where the preferred chair-chair-conformation of the intermediate is easily accessible (Setzer, 2008; Adio, 2009). One example, however, with Cope rearrangement of a *cis*-fused germacranolide is described. In this example, also only one product is formed in high yield (Appendino and Gariboldi, 1983).

The biochemical lactone ring reaction observed here is also known from Asteraceae where the biosynthesis of (+)-costunolide follow the same type of reaction. In order to establish the lactone ring in (+)-costunolide, two P450s are needed. First three consecutive hydroxylations are performed on C-12 by one P450 (GAO), generating germacra-1(10),4,11(13)-trien-12-ol followed by germacra-1(10),4,11(13)-trien-12-al and resulting in germacra-1(10),4,11 (13)-trien-12-oic acid (Nguyen et al., 2010; Cankar et al., 2011; Liu et al., 2011; Ramirez et al., 2013; Eljounaidi et al., 2014; Liu et al., 2014) (Figure 7). A second P450 (COS) hydroxylates germacra-1(10),4,11(13)-trien-12-oic acid at C-6, resulting in spontaneous lactone formation (Ikezawa et al., 2011; Liu et al.,

2011; Ramirez et al., 2013; Eljounaidi et al., 2014). The lactone formation in *T. garganica* is simpler than the formation reported in the Asteraceae species, since epikunzeaol already has a hydroxyl group at C-6 and therefore only requires one P450. Thus, the triple oxidation on C-12 to the carboxylic acid leads to a spontaneous lactone ring formation. Consequently, it is not possible to detect the intermediates that are expected to be an alcohol, aldehyde and acid. The suggested mechanism of epidihydrocostunolide biosynthesis in Figure 7 is based on the previously described mechanism for costunolide in Asteraceae (Nguyen et al., 2010; Cankar et al., 2011; Ikezawa et al., 2011; Liu et al., 2011; Ramirez et al., 2013; Eljounaidi et al., 2014).

Neither of the two enzymes CYP71BL1 (GAO) and CYP71BL2 (COS) which, catalyze 8β- and 6α-hydroxylation of germacrene A acid, respectively, shows high identity to *Tg*CYP76AE2 with 32.2 % for GAO and 36.6 % for COS (Ikezawa et al., 2011). This is despite Apiaceae and Asteraceae are closely related families, exemplifying limitations with prediction of CYP functionality based on phylogenetic relationship.Sesquiterpenoid lactones are a broad class of compounds and other mechanisms for formation of a lactone ring have been reported. The biosynthesis of the lactone ring in the sesquiterpenoid artemisinin for instance is different to what is found for (+)-costunolide and epidihydrocostunolide. Here an aldehyde dehydrogenase and an aldehyde reductase are involved in addition to a P450. These jointly participate in the formation of an acid that is then non-enzymatically converted into the lactone ring, as opposed to the (+)-costunolide and dihydrocostunolide biosynthesis where ring formation is achieved solely by P450 catalysis (Teoh et al., 2006; Liu et al., 2011)

The P450s, GAO and COS, from Asteraceae that catalyze the lactone ring formation in (+)-costunolide are from the CYP71 family. While the CYP71 family of the CYP71 clan has had much focus, the CYP76 family is now emerging as another major participant in the biosynthesis of specialized metabolites especially terpenoids. CYP76's have been found to participate in both mono- sesqui- and diterpenoid biosynthesis (Collu et al., 2001; Guo et al., 2013; Weitzel and Simonsen, 2015). In sesquiterpenoid biosynthesis, CYP76F has been described in *Santalum album* as part of the santalol and bergamotol biosynthesis (Diaz-Chavez et al., 2013; Celedon et al., 2016). The CYP71 clan is becoming more of a continuum and it is expected that future sequencing will add to this and make it even harder to distinguish between the families and subfamilies of this clan. Investigation of P450s involved in sesquiterpenoid metabolism are expanding from the CYP71 family to the CYP71 clan, as seen in Figure 2, and in the future probably also beyond that.

Stereochemistry and non-conjugation

A characteristic difference between the guaianolides from Asteraceae and Apiaceae, like thapsigargin, is the α-disposal of the C-6-O bond in Asteraceae whereas it is β-disposed in Apiaceae (Simonsen et al., 2013). The present study support that the β-C-6-O bond characteristic for thapsigargin is introduced already at the very first step of sesquiterpenoid biosynthesis with the formation of epikunzeaol. *Tg*CYP76AE2 converts epikunzeaol to epidihydrocostunolide, which differs from dihydrocostunolide by the β-disposed C-6-O bond. Since no epimerization of C-6 is likely under the oxidative transformation of C-12 into a carboxylic acid the previous suggested structure of epikunzeaol as the 6α-hydroxygermacrene must be considered unlikely (Pickel et al., 2012). The suggested structure was only based on assignment of major signals in the spectrum, which might explain the erroneous assignment of stereochemistry.

The expression of genes, involved in sesquiterpene biosynthesis, in *N. benthamiana* has previously been reported to result in glycosylation or other conjugations of the produced sesquiterpenoids. For artemisinic acid in the artemisinin pathway, it was seen that this was conjugated to a diglucoside (van Herpen et al., 2010). When the genes in the costunolide biosynthesis was expressed in *N. benthamiana* costunolide was conjugated to glutathione or cysteine (Liu et al., 2011). Analysis of products of *Tg*CYP76AE2 did not reveal any conjugation and were therefore detectable by GC-MS. In contrast to costunolide, epidihydrocostunolide does not possess a C-11-C-13 double bond preventing a conjugation to a thiol group.

Downstream pathway towards thapsigargin

Costunolide has been suggested as a precursor of many of the studied sesquiterpene lactones in the Asteraceae (de Kraker et al., 2002). The finding of a P450 from *T. garganica*, which synthesizes epidihydrocostunolide, indicates that epidihydrocostunolide could have a similar role in *Thapsia* and that the unusual stereochemistry at C-6 is introduced at a very early stage. Further modification of epidihydrocostunolide to produce thapsigargin would require a mechanism to produce a 5- and 7-ring closure of the 10-membered ring of epidihydrocostunolide. The exact reaction and enzyme responsible are yet unknown. A putative route could be the oxidation mediated ring closure similar to what has been described for the biosynthesis of lathyranes in *Euphorbiacae* species (Luo et al., 2016). Furthermore, several hydroxylations and various acetylations of the backbone are required. A number of these reactions are likely to be performed by P450s.

Specialized tissue for storage of sesquiterpenoids

Terpenoids are often located in specialized storage structures in plants, which include oil glands, secretory ducts, laticifers, trichomes and vacuoles (Fahn, 1988; Chadwick et al., 2013). Cells adjacent to or harboring these compartments have been shown to be involved in the biosynthesis of terpenoids that are then transported into the storage compartment (Olsson et al., 2009; Lange, 2015). *T. garganica* is closely related to the genus *Daucus* and has a taproot like carrots (Weitzel et al., 2014). In carrots, it was shown that lipophilic compounds including specialized metabolites were primarily localized in extracellular, long schizogenous hydrophobic oil ducts that were located in the periderm/pericyclic parenchyma tissue (Esau, 1940; Schuphan and Boek, 1960; Deutschmann, 1969; Garrod and Lewis, 1980). The secretory ducts in *Daucus* are highly organized and connected throughout the phloem of roots and exhibit a concentric ring pattern in horizontal sections (Deutschmann, 1969; Bowes and Mauseth, 2008). Likewise, a positive correlation between the number of ducts and amount of terpenoids has been demonstrated (Garrod and Lewis, 1980; Senalik and Simon, 1986).

NADI was chosen as a possible stain for terpenoids. The use of NADI has been known since the 1880's and has since been used to detect oxidized compounds. David and Carde, 1964 were the first to report the use of NADI for staining of terpenoids, unfortunately the exact mechanism nor the specificity were described. Throughout the years, the exact mechanism has been much debated and the specificity for terpenoids is still uncertain. NADI does however, function as a useful method in the current setting to visualize secretory ducts whether the stain is specific towards oxidized and/or lipophilic compounds, including terpenoids.

The finding that transcripts from *Tg*TPS2 and *Tg*CYP76AE2 are exclusively found in epithelial cells surrounding secretory ducts in the middle part of the root supports their involvement in the biosynthesis of thapsigargin. Intermediates from the biosynthesis of thapsigargin were not identified in extracts from *T. garganica* in this study nor in previous studies. This could signify a specific and efficient or possibly even a channeled biosynthetic pathway indicating metabolon formation of the enzymes (Møller, 2010). The presence of thapsigargin in highly specific locations also supports the function of ducts as storage compartments in the roots, and possibly also ducts in the fruits of *T. garganica,* which might explain the high content in these two organs. Similar observations were made in stem cross-sections from the conifer *Picea sitchensis* upon methyl jasmonate treatment (Zulak and Bohlmann, 2010). An antibody against the diterpene synthase, levopimaradiene/abietadiene synthase allowed detection of a fluorescence signal in the epithelial cells of cortical and traumatic resin ducts 2 days after methyl jasmonate treatment. In addition, this

indicated the importance of these epithelial cells in the biosynthesis of specialized metabolites. In a following study in *Picea sitchensis* the importance of the epithelial cells were further implemented (Abbott et al., 2010; Hamberger et al., 2011). Here epithelial cells were isolated with laser micro-dissection, studied by RT-qPCR and found to be enriched in a variety of CYP720s including PsCYP720B4 involved in biosynthesis of isopimaric acid and abietic acid. This approach is of high relevance to the further elucidation of the thapsigargin biosynthetic pathway.

Focus in the present study has been directed towards localizing specific tissue in *T. garganica*, which could biosynthesize and store sesquiterpenoids such as thapsigargin. As it was previously shown that the amount of secretory ducts correlate with the amount of terpenoids and especially lipophilic terpenoids, cells lining these are an obvious target for biosynthesis studies (Senalik and Simon, 1986). The finding that thapsigargin is stored in secretory ducts in the roots and the enzymes involved in the biosynthesis are present in the surrounding cells opens up new possibilities. The data presented here suggest that future studies, including identification of enzymes involved in specialized metabolism and specialized transporters in the cells lining the secretory ducts would benefit from the transcriptomics of these.

Conclusion

The roots of the Mediterranean plant *Thapsia garganica* (dicot, Apiaceae), also known as Deadly carrot, have been shown to have secretory ducts that likely contain the highly toxic compound thapsigargin and similar sesquiterpenoid lactones. Through transient expression of *Tg*TPS2 (epikunzeaol synthase) and *Tg*CYP76AE2 in *Nicotiana benthamiana* it was shown that *Tg*TPS2 (epikunzeaol synthase) and *Tg*CYP76AE2 converts epikunzeaol into epidihydrocostunolide, compounds which are possible intermediates in thapsigargin biosynthesis. Transcripts from *Tg*TPS2 (epikunzeaol synthase) and *Tg*CYP76AE2 were found in the epithelial cells lining the secretory ducts and nowhere else in the root. This emphasizes the involvement of these specific cells in the biosynthesis of thapsigargin and other sesquiterpene lactones in *T. garganica*.

The findings presented here enable the full elucidation of the biosynthesis of thapsigargin biosynthesis in the cells lining the secretory ducts. The findings also show the power of *in situ* PCR combined with MALDI-TOF imaging.

Materials and Methods

Plant material

Thapsia garganica L. roots used for cDNA synthesis to obtain genes of interest were collected in June 2010, 25 km SSW of Bari, Italy (GPS 40.898625, 16.706139).

For NADI staining, in tube *in situ* PCR and MALDI-MSI 2 year old *T. garganica* plants were used. These had been grown in Ibiza, and were purchased from ThapsIbiza S. L.

Identification and cloning of genes

The ORF of P450s belonging to the CYP71 clade was found in the transcriptome of the *Thapsia garganica* root (SRX096991) (Pickel et al., 2012) based on BLAST searches using a set of CYP71 clan members as previously described (Dueholm et al., 2015). The P450s are available on NCBI; *TgCYP71AH8* (KX826939), *TgCYP71AS14* (KX845553), *TgCYP71AT12* (KX826940), *TgCYP71AU89* (KX845548), *TgCYP71AU90* (KX845552), *TgCYP71BK1* (KX826941), *TgCYP71BK6* (KX845546), *TgCYP71D183* (KX845554), *TgCYP71D311* (KX845555), *TgCYP71D319_ortholog* (KX845550), *TgCYP76AE1* (KX826942), *TgCYP76AE2* (KX826943), *TgCYP76AE8* (KX845545), *TgCYP76AF7* (KX845549), *TgCYP76B79* (KX845547) and *TgCYP706C30_ortholog* (KX845551). *TgCYP71AJ5* (KP191555) and *TgCYP71AJ14* (KP191558) were also tested previously (Dueholm et al., 2015). The discovery of *TgTPS2* (JQ290345) has been described in (Pickel et al., 2012). Full-length gene sequences were obtained from a cDNA library of *T. garganica* root material.

Forward and reverse primers for all genes were designed with USER-overhangs, to enable cloning into a pEAQ USER compatible version of the pEAQ-*HT* vector (Table S1,) (Luo et al., 2016). pEAQ-*HT* harbors the viral suppressor p19 and was kindly provided by George Lomonosonoff (John Innes Research Centre, Norwich, UK) (Peyret and Lomonossoff, 2013). USER cloning was performed as depicted previously (Nour-Eldin et al., 2006). A truncated version of *Arabidopsis thaliana* HMGR (GenBank J04537), described previously (Cankar et al., 2015), was kindly provided Katarina Cankar (Wageningen University, The Netherlands).

*Tc*CYP71AV2 (KC441527.1), *Ci*CYP71AV8 (HQ166835.1), *Cc*CYP71AV9 (KF752448.1), *Ls*CYP71BL2 (HQ439599.1), *Ci*CYP71BL3 (JF816041.1), *Tc*CYP71BL4 (KC441528.1) and *Cc*CYP71BL5 (KF752451.1) were furthermore blasted into the *T. garganica* root transcriptome. Setting the expectation value to 1E-100 no hits were available.

Phylogeny

In total 53 full-length sequences of functional characterized cytochromes P450 related to sesquiterpenoid biosynthesis and cytochromes P450 from *T. garganica* were used to build the phylogenetic tree. The full list is in the supplementary file as part of the alignment, and the NCBI numbers for the *Thapsia* genes are given above.

All obtained full length sequences were aligned using default options in MUSCLE and ClustalW (Edgar, 2004), as implemented in the software Geneious 10.0.5 (www.geneious.com) followed by manual modification. Phylogenetic analyses were conducted using maximum likelihood. Default options for PhyML based on the substation model LG, in Geneious 10.0.5 was chosen (Guindon et al., 2010). All maximum likelihood trees (ML) were obtained using 1,000 replicates of random taxon addition sequence. All characters were included in the analyses. Clade support was assessed using non-parametric bootstrap re-sampling. Bootstrap analysis (Felsenstein, 1985) was carried out using 1,000 replicates. We defined bootstrap percentages (BS) < 50 % to be unsupported, between 50 % and 74 % as weak support, between 75 % and 89 % BS as supported, and scores of greater than 90 % BS as strong support. Alignments supporting the tree are given in supplementary file 1 (for Figure 2). The *Thapsia* gene cinnamate-4-hydroxylase (*Tg*C4H) was used to root the tree.

Expression of *Tg*TPS2 and P450s in *Nicotiana benthamiana*

N. benthamiana plants were grown from seeds at 24°C/19°C (day/night) for five weeks before transformation. The transformation of *Agrobacterium tumefaciens* and infiltration of *N. benthamiana* with *A. tumefaciens* followed the protocol described by (Bach et al., 2014). In short, 10 ml LB containing kanamycin, rifampicin and carbenicillin was inoculated with several agrobacterium colonies containing the plasmid of interest. Cultures were grown ON at 28°C and 200 rpm. Cell pellets were washed twice with water before final resuspension in water followed by a dilution to OD_{600} 0.5. Resuspended *A. tumefaciens* carrying plasmids containing *At*tHMGR, *Tg*TPS2 or *Tg*CYPs were mixed 1:1:1 and infiltrated into leaves of at least three *N. benthamiana* plants by use of a syringe. Plants were placed at 24°C/19°C (day/night) and harvested five days after infiltration. As controls, plants were infiltrated with *A. tumefaciens* carrying plasmids with no additional genes, *At*tHMGR, and *At*tHMGR plus *Tg*TPS2.

The ~100 plants needed for purification of products **1**, **2** and **3** were infiltrated by use of vacuum. Three *A. tumefaciens* cultures containing *At*tHMGR, *Tg*TPS2 or *Tg*CYP76AE2 were grown ON at 28°C and 200 rpm in 500 ml LB (containing kanamycin, rifampicin and carbenicillin) from 20 ml

starter cultures. Cell pellets were washed twice with water before final resuspension in water followed by a dilution to OD_{600} 0.5. Resuspended *A. tumefaciens* carrying plasmids containing *At*tHMGR, *Tg*TPS2 or *Tg*CYP76AE2 were mixed 1:1:1. Plants were submerged in a 1 L suspension of *A. tumefaciens* and infiltrated by use of vacuum at 50-100 mbar for 1 min (Andersen-Ranberg et al., 2016).

GC-MS detection of sesquiterpenoids

Two leaf discs (Ø=3cm) from *N. benthamiana,* expressing genes from *T. garganica* were extracted with 1.2 ml hexane for GC-MS analysis to provide one sample, a minimum of three biological replicates were examined.

Hexane extracts were analyzed on a Shimadzu GCMS-QP2010 using an Agilent HP-5MS UI, 20 m, 0.18 mm diameter × 0.18 µm film thickness column kept at a pressure of 66.7 kPa giving a column flow of 1 mL/min(Drew et al., 2012). The injection port temperature was set to 160°C or 250°C to find the optimal temperature (Andersen et al., 2015). The oven temperature was set to 60°C for 3 min, and then increased to 160°C with a rate of 7°C/min. The temperature was further increased to 300°C at a rate of 50°C/min, held for 5 min, finally increased to 320°C at 50°C/min and maintained for 3 min. The carrier gas was H_2 and the ionization electron energy was 70 eV. The ion source temperature was 230°C with an interface temperature 280°C. The total run time was 11.67 min. All data were analyzed using the Shimadzu software Lab Solutions, GCMS Solutions version 2.50 SU3, with the 2008 libraries provided by NIST and Wiley.

Analytical LC-MS for detection of novel sesquiterpenoids

Two leaf discs with a diameter of 3 cm were ground in liquid nitrogen to provide one samples, a minimum of three biological replicates was examined. Samples were extracted with 1200 µl 80 % methanol and sonicated for 30 min. Before LC-MS analysis samples were filtered through a 0.45 µm filter. Analytical LC-MS was carried out using an Agilent 1100 Series LC (Agilent Technologies, Germany) coupled to a Bruker HCT-Ultra ion trap mass spectrometer (Bruker Daltonics, Bremen, Germany). A Gemini-NX column (Phenomenex; 3 µm, C18, 110A, 2 × 150 mm) maintained at 35°C was used for separation. The mobile phases were; A, water with 0.1 % (v/v) formic acid; B, acetonitrile with 0.1 % (v/v) formic acid. The gradient program was: 0 to 1 min, isocratic 12 % B; 1 to 33 min, linear gradient 12 to 80 % B; 33 to 35 min, linear gradient 80 to 99 % B; 35 to 38 min, isocratic 99 % B; 38-47 min, isocratic 12 % B. The flow rate was 0.2 ml min^{-1}. The mass spectrometer was run in positive mode and the mass range *m/z* 100-1000 was acquired.

Preparative GC-MS - purification of Cope rearranged sesquiterpenoids (2 and 3)

For isolation of compounds **2** and **3**, a large-scale hexane extraction was made from *N. benthamiana* leaves expressing *At*tHMGR, *Tg*TPS2 and *Tg*CYP76AE2. The leaves from approximately 130 five-week-old plants were used. The sample was subjected to an initial separation on a silica column and eluted with hexane:ethyl acetate at 13% ethyl acetate. The final purification was done on an Agilent 7890B GC installed with an Agilent 5977A inert MSD, GERSTEL Preparative Fraction Collector (PFC) AT 6890/7890 and a GERSTEL CIS 4C Bundle injection port. For separation by GC, a RESTEK Rtx-5 column (30 m × 0.53 mm ID × 1 μm d_f) with H_2 as the carrier gas was used. At the end of this column was a split piece with a split of 1:100 to the MS and the PFC, respectively. A sufficient amount of sesquiterpene product for NMR analysis (0.5-1 mg) was obtained by 100 repeated injections of 5 μL of extract. The injection port was put in solvent vent mode with a carrier gas flow of 100 mL/min until 0.17 min. This was combined with an injection speed of 1.5 mL/min. The purge flow was set to 3 mL/min from 0.17 min to 2.17 min. The injection temperature was held at 40°C for 0.1 min, followed by ramping at 12°C/sec until 320°C, which was held for 2 min. The column flow was set to 7.5 mL, which was held constant throughout the GC program. The GC program was set to hold at 60°C for 1 min, ramp 20°C/min to 320°C, which was held for 3 min. Temperature of the transfer line from GC to PFC and the PFC itself was set to 250°C. The PFC was set to collect the peak of product **2** and **3** by their retention time identified by the MS. The MS was set in scan mode from *m/z* 35 to *m/z* 500, with a threshold of 150. Solvent cut-off was set to 4 min, and the temperature of the MS source and the MS quadrupole was set to 300°C and 150°C, respectively. Traps were kept at -20°C and rinsed with chloroform-d (Euriso-top, 99.8 atom % D).

Purification of epidihydrocostunolide (1)

For isolation of compound **1**, a large-scale hexane extraction was made from *N. benthamiana* leaves expressing truncated *At*HMGR, *Tg*TPS2 and *Tg*CYP76AE2. The leaves from approximately 100 five-week-old plants were used. The crude hexane extract was subjected to an initial preparative separation on a Biotage Isolera autoflasher using a 10 g, 50 μm diol column and eluted stepwise with hexane to hexane:ethyl acetate (80:20) with 2 % increaments of ethyl acetate. Final isolation of **1** was achieved by semi-preparative HPLC on a 250 × 10 mm, 7 μm Nucleosil PEI column (Macherey-Nagel) eluted isocratic with hexane on a Waters 600 HPLC equipped with a Waters 996 PDA detector.

576 **^{1}H and ^{13}C NMR spectroscopic analysis**

577 NMR-spectra were acquired using a 600 MHz Bruker Avance III HD NMR spectrometer (^{1}H
578 operating frequency 600.13 MHz) equipped with a Bruker SampleJet sample changer and a
579 cryogenically cooled gradient inverse triple-resonance 1.7-mm TCI probe-head (Bruker Biospin,
580 Rheinstetten, Germany) optimized for ^{13}C and ^{1}H. Samples were analyzed at 300 K. Proton spectra,
581 at 600.03 MHz, were obtained using 30°-pulses, a spectral width of 12 kHz, collecting 16 scans
582 with a length of 65536 data points with a relaxation delay of 1.0 sec. Carbon spectra were acquired
583 at 150.88 MHz with 30°-pulses, a spectral width of 36 kHz, collecting 256 scans with a length of
584 65536 data points and with a relaxation delay of 2.0 sec. The ^{13}C nuclei were ^{1}H-decoupled using
585 the Waltz-16 composite pulse-decoupling scheme. FID's were exponentially multiplied with a line-
586 broadening factor of 1.0 Hz before Fourier transformation. The 2D experiments were recorded
587 using Bruker standard parameter settings. The isolated product **1** was dissolved in MeCN-d_3 (99.8
588 atom % D), while **2** and **3** were dissolved in $CDCl_3$ (99.8 atom % D) prior to NMR analysis.

589 **Histochemical analysis staining**

590 Taproots (~ 2 cm in diameter) were dug up just prior to sectioning. Cross-sections of roots were cut
591 in 60 µm thick sections with a vibratome (Microm, HM 650 V). Histochemical analysis was
592 performed with NADI reagent (1% naphthol + 1% dimethyl-p-phenylenediamine + 0.05M
593 phosphate buffer, pH 7.2) reported to stain terpenoids blue (David and Carde, 1964). Sections were
594 immersed in phosphate buffer 0.05 M (pH 7.2) buffer or NADI solution immediately after cutting
595 and left for minimum 30 min before analysis. Samples were mounted on glass slides and images of
596 the sections were obtained under a Leica DMR HC microscope through x20, x40 dry objectives and
597 an x100 oil immersion objective.

598 **MALDI-MSI**

599 Prior to MALDI analysis, thapsigargin had been verified to be present in the roots by HPLC as
600 previously described (Christensen et al., 1984; Pickel et al., 2012).

601 **Tissue preparation** Root tissue was snap-frozen in a cooling bath (2-propanol:dry-ice) and tissue
602 blocks from the middle part of the root were mounted to the chuck using Tissue-Tek® O.C.T.
603 compound. Tissues were sectioned on a cryosectioner (Leica 3050S cryostat). Sections were cut to
604 60 µm thick, ensuring no O.C.T. came into contact with the sectioned tissue. Sections were
605 transferred onto pre-chilled Menzel-Gläser Superfrost Plus 25 mm × 75 mm × 1.0 mm glass slides
606 and gently adhered to pre-mounted double-sided adhesive carbon tape (Agar Scientific, UK). The

frozen slide with sections was transferred into a chilled 50 mL falcon tube then freeze dried for 24h using a freeze dryer (ScanVac CoolSafe), set to −95°C and an operating pressure of 1 mBar. Samples were stored in a vacuum desiccator prior to matrix deposition.

Matrix Deposition Matrix, 2,5-dihydroxybenzoic acid (DHB) was sublimed onto tissue sections using a custom built sublimation apparatus at temperatures of 130-140°C, at vacuum pressures less than 0.1 mBar for a period of 15 minutes generating a matrix coverage of 0.3 ± 0.1 mg/cm^2. An ice slurry was used to cool the sample cold finger. Alternatively, DHB was deposited onto tissues by spray deposition using a HTX Imaging TM Sprayer (HTX Technologies). DHB in acetone/water (50 mg/mL, 95:5) was sprayed at 30°C using 4 passes, a solvent flow rate of 150 µL/min, a nozzle velocity of 1200 mm/min, with alternate passes at 90° offset, 2 mm track spacing and 1 mm offset for repeat passes, nitrogen sheath gas pressure was set to 10 psi. After deposition, samples were then stored in a desiccator prior to analysis.

Optical Image Optical images of tissue sections were acquired using an EPSON Photosmart 4400 flatbed scanner using EPSON Scan Version 3.04A with a setting of 4800 d.p.i.

Mass Spectrometer For spatial mass spectrometric analysis, a SolariX XR 7 Tesla Hybrid ESI / MALDI FT-ICR-MS (Bruker Daltonik) was used. The instrument was operated in the Positive ion mode using optimized instrumental settings across the mass range 100-2000 *m/z*, with the instrument set to Broadband mode with a Time Domain for Acquisition of 2M providing an estimated resolving power of approximately 260000 at 400 *m/z* using a total of 1 ICR cell fills. The instrument was calibrated to less than 1 ppm tolerance against elemental Red Phosphorous clusters using a Quadratic calibration curve across the mass range 216-1951 *m/z*. The laser was set between 38-50 % power using the minimum spot size with Smart Walk enabled using a width of 40 µm, grid increment of 10 and offset of 1 using a random walk pattern resulting in ablation spots of approximately 40-50 µm in diameter. A total of 500-750 shots were fired per spectra at a frequency of 2 KHz within a 50 × 50 µm array.

Data Analysis Acquired mass spectrometry data was analysed using Compass FlexImaging 4.1 (Build 116, Bruker Daltonik GmbH). Images were either normalized to Root Median Square (RMS) or Total Ion Chromatogram (TIC) and brightness optimization employed to enhance visualization of the distribution of selected compounds. Individual spectra were analyzed and recalibrated using Bruker Compass DataAnalysis 4.3 (Build 110.102.1532) to internal lock masses of known DHB clusters; $C_{14}H_9O_6$ = 273.039364 and $C_{21}H_{13}O_9$ = 409.055408 *m/z*. Peak lists were generated using S/N threshold = 4 and 0.15 % base peak height threshold.

In tube *in situ* RT-PCR on root tissue sections

The *in situ* PCR was performed as previously described (Athman et al., 2014), with some modifications. Root tissue was left for 4 hours in ice cold FAA. 75µm thick root cross-sections were cut with a vibratome and transferred into tubes containing, RNAsin (Promega, N2515) as the RNase inhibitor. A DNase treatment with DNAse 1 and 10x Turbo DNAse (Qiagen 79254) was extended to overnight at 37°C. Sections were incubated for 15 min in 0.5M EDTA at 70°C, rinsed with ice cold nuclease free water then incubated on ice for 15 min in 2mg Pepsin in 0.1M HCl prior to the reverse transcription step to remove cross-linking. Reverse transcription was carried out using the Sensicript Reverse Transcription Kit (Qiagen 205213). The first cycling conditions were 5 min at 65°C followed by 1 min at 4°C. RNAsin and the reverse transcriptase enzyme were then added and the following cycling parameters used: 60 min at 42°C, 95°C for 5min, 1 min at 4°C for 1 min and the tubes were then placed directly on ice. The *in situ* PCR followed using TaKaRa Ex Taq (Clontech, RR001A), 5mM dNTPs and PCR DIG labelling mix (Sigma-Aldrich, 11585550910) in the PCR solution.

The negative controls followed the preparation of the test samples, but with the reverse transcriptase enzyme omitted. A positive control was carried out with the ribosomal 18S transcript. The primers used for the cDNA synthesis step [reverse (R) only] and PCR [forward (F) and reverse] are listed in Table S2; the products amplified by these primers were sequenced to confirm their specificity. The cycling parameters were: initial denaturation at 95°C for 2 min, 40 cycles of 95°C for 10 sec, X°C for 30 sec, 72°C for 1 min (X = 58°C for *Tg*CYP76AE2, 56°C for *Tg*TPS2 and 18S). The final extension was at 72°C for 5 min and then held at 4 °C. Sections were incubated on ice for 30 min in a blocking solution (1% bovine serum albumin in 1X phosphate buffer) to prevent background staining. Anti-DIG-AP Fab fragments were then added followed by a 60 min incubation at room temperature. BM purple AP substrate (Sigma-Aldrich, 000000011442074001) was used for colorimetric staining. Sections were stained for 1.5 hours and mounted in Antifading solution (Citifluor, AF3-25). Slides were viewed with a Leica DMR HC microscope.

Acknowledgements

George Lomonosonoff (John Innes Research Centre, Norwich, UK) provided the pEAQ-*HT* plasmid. Katarina Cankar provided the truncated HMGR (Wageningen University, Wageningen, The Netherlands). MALDI MSI was conducted at Metabolomics Australia (School of BioSciences, The University of Melbourne, Australia), a NCRIS initiative under Bioplatforms Australia Pty Ltd.

670

671 (Figure 8)

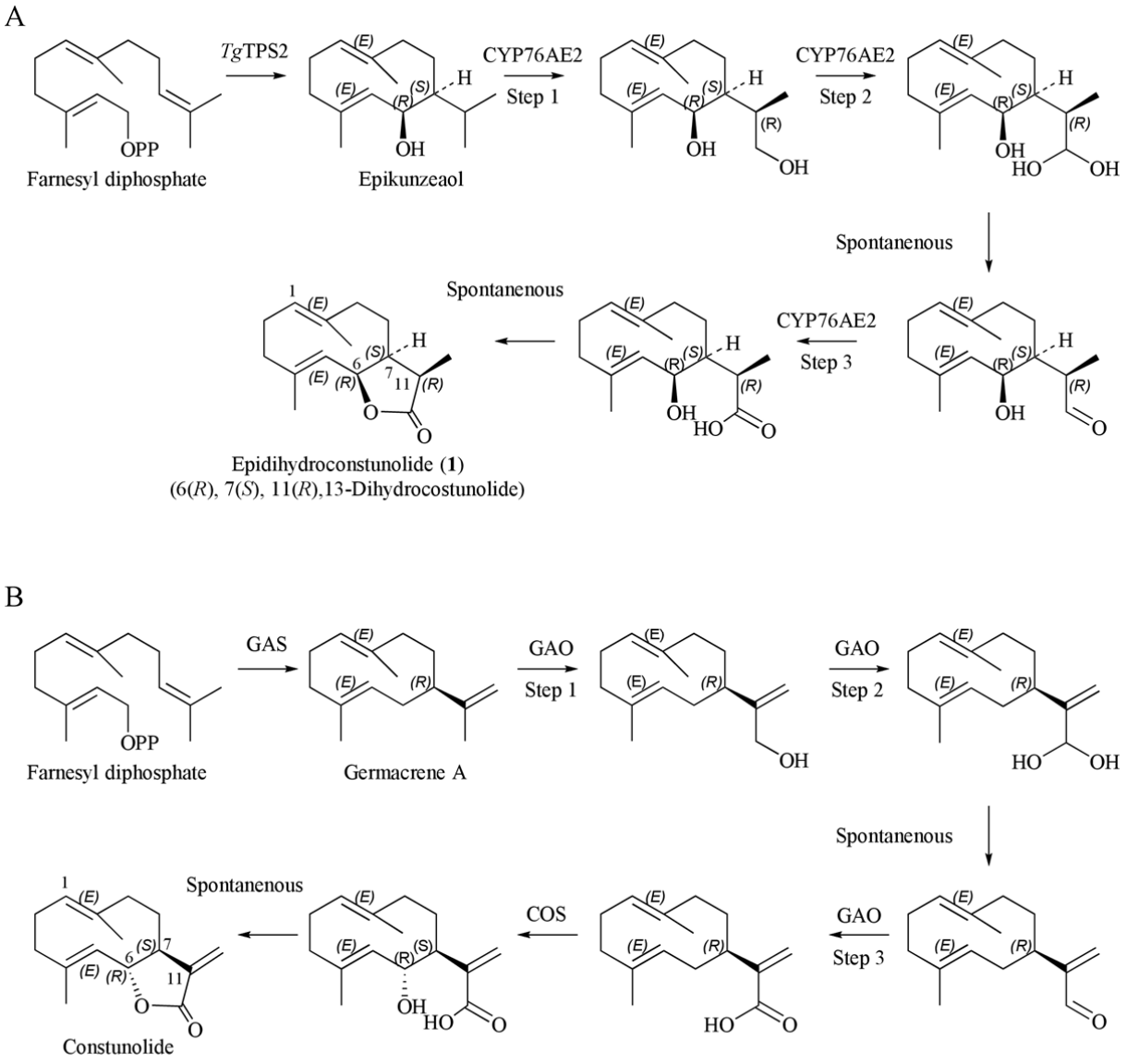

Figure 8 A: Proposed biosynthesis of **1**. *Tg*CYP76AE2 is suggested to catalyze three hydroxylations to obtain epidihydrocostunolide. The intermediates are based on knowledge from the costunolide pathway. **B:** The costunolide pathway is as follows. Step one is GAS (germacrene A synthase (Bouwmeester et al., 2002)) followed by three consecutive hydroxylation's by GAO (germacrene A oxidase, CYP71AV2-9, (Nguyen et al., 2010; Cankar et al., 2011; Ramirez et al., 2013; Eljounaidi et al., 2014)). Finally, a one hydroxylation of C6 by COS (costunolide synthase, CYP71BL2-5, (Ikezawa et al., 2011; Liu et al., 2011; Ramirez et al., 2013; Eljounaidi et al., 2014)) to yield costunolide.

Table 1: ^{13}C NMR results for **1**, **2** and **3**. Samples were analyzed at 300 K. The isolated product **1** was dissolved in MeCN-d_3 (99.8 atom % D), while 2 and 3 were dissolved in $CDCl_3$ (99.8 atom % D).

	1	**2**	**3**
#C	δ_C (ppm)	δ_C (ppm)	δ_C (ppm)
1	128.7	148.7	147.2

2	26.4	110.9	111.2
3	40.6	116.4	114.4
4	137.7	143.5	144.6
5	127.1	54.8	51.9
6	79.3	81.2	81.2
7	46.2	40.6	37.2
8	23.7	18.6	18.9
9	37.7	37.6	32.1
10	139.4	39.0	37.7
11	41.5	41.3	40.6
12	180.6	179.3	178.9
13	10.9	9.2	10.2
14	22.2	18.6	25.5
15	17.4	26.0	26.1

675

676

677 **Table 2**. ^{1}H NMR results for **1**, **2** and **3**. Samples were analyzed at 300 K. The isolated product 1
678 was dissolved in MeCN-d_3 (99.8 atom % D), while 2 and 3 were dissolved in $CDCl_3$ (99.8 atom %
679 D).

	1	**2**	**3**
#H	ppm δ_H (*J* in Hz)	ppm δ_H (*J* in Hz)	ppm δ_H (*J* in Hz)
1	5.00 m, overlaid	5.80 dd, *J*=17.5, 10.8 Hz, 1 H	5.93 dd, *J*=17.6, 11.0 Hz, 1 H
2a	2.10 m, overlaid H	4.97 d, *J*=10.5 Hz, 1 H	4.98 d, *J*=17.2 Hz, 1 H
2b	2.27 m, overlaid H	4.98 d, *J*=18.0 Hz, 1 H	4.99 d, *J*=11.7 Hz, 1 H
3a	2.04 m, overlaid H	5.02 s, 1 H	4.85 s, 1 H
3b	2.23 m, overlaid H	5.07 s, 1 H	4.99 s, 1 H
5	4.98 d, *J*=10.1, overlaid H	2.13 d, *J*=2.6 Hz, 1 H	2.56 d, *J*=4.0 Hz, 1 H
6	5.14 dd, *J*=9.8, 4.6, 1H	4.45 t, *J*=3.3 Hz, 1 H	4.50 t, *J*=4.8 Hz, 1 H
7	2.49 m, overlaid H	2.29 - 2.36 m, 1 H	2.57 - 2.65 m, 1 H
8	1.59 s		
8a		1.37 qd, *J*=13.9, 2.90 Hz, 1 H	1.42 - 1.52 m, 1 H
8b		1.64 ddd, *J*=13.5, 6.3, 3.3 Hz, 1 H	1.61 - 1.67 m overlaid, 1 H
9			1.56 - 1.61 m overlaid, 2 H
9a	1.70 m, overlaid H	1.55 m, overlaid H	
9b	2.45 d, *J*=13.0, 1H	1.53 m, overlaid H	
11	2.94 m, overlaid H	2.76 quin, *J*=7.0 Hz, 1 H	2.79 quin, *J*=7.3 Hz, 1 H
13	1.13 s, 3H	1.21 d, *J*=7.3 Hz, 3 H	1.22 d, *J*=7.3 Hz
14	1.53 s, 3H	1.20 s, 3 H	1.03 s, 3 H
15	1.67 s, 3H	1.87 s, 3 H	1.85 s, 3 H

680
681

682 **Table 3.** Calculated and observed masses (incl. error expressed in ppm) of Na and K adducts of
683 thapsigargin, epikunzeaol, epidihydrocostunolide and a selection of known guaianolides from *T.*
684 *garganica* in the MALDI experiment.

		$[M+Na]^+$			$[M+K]^+$		
Compound	Mol. Form.	Calc.	Obs.	Error	Calc.	Obs.	Error
Epikunzeaol	$C_{15}H_{26}O$	245.18759	-	-	261.16152	-	-
Epidihydrocostunolide	$C_{15}H_{22}O_2$	257.15120	-	-	273.12514	-	-
Nortrilobolide	$C_{26}H_{36}O_{10}$	531.22007	531.22110	-1.94	547.19401	547.19380	0.38
Trilobolide	$C_{27}H_{38}O_{10}$	545.23572	545.23370	3.70	561.20966	561.20730	-0.01
Thapsivillosin L	$C_{30}H_{42}O_{12}$	617.25685	-	-	633.23079	633.23240	-2.55
Thapsivillosin I	$C_{31}H_{42}O_{12}$	629.25685	629.25830	-2.31	645.23079	645.2327	-2.97
Thapsivillosin J	$C_{31}H_{44}O_{12}$	631.27250	-	-	647.24644	-	-
Thapsigargicin	$C_{32}H_{46}O_{12}$	645.28815	645.2864	2.71	661.26209	661.26040	-0.01
Thapsigargin	$C_{34}H_{50}O_{12}$	673.31945	673.3186	1.26	689.29339	689.2924	1.43
Thapsivillosin C	$C_{35}H_{52}O_{12}$	687.34588	-	-	703.30904	-	-

685
686
687
688 SUPPLEMENTAL DATA
689
690 Supplemental Table 1. Primers for cloning into the USER version of the vector pEAQ.
691 Supplemental Table 2. In tube *in situ* primers.
692 Supplemental Figure 1. ^{13}C and ^{1}H NMR spectra of product 1, 2 and 3.
693 Supplemental Figure 2. Cope-rearrangement of 1 upon GC-MS analysis.
694 Supplemental Figure 3. MALDI-MSI analysis of *T. garganica* taproot section and structures of
695 metabolites.
696 Supplemental Figure 3-2. MALDI-MSI analysis of *T. garganica* taproot section.
697 Supplemental Figure 4. Alignment for the figure 2 tree.
698
699

700 **Figure legends**

701

702 **Figure 1.** The structure of epikunzeaol and epidihydrocostunolide (**1**). Both metabolites are
703 suggested intermediates in the thapsigargin pathway in *T. garganica*.

704

705 **Figure 2:** The tree shows the phylogeny of P450s from *Thapsia garganica* (within CYP71 clade)
706 and cytochromes related to sesquiterpenoid biosynthesis. The notes with *Thapsia* genes are marked
707 in blue. The only two groups in the tree that can be assigned to a biochemical function are the
708 germacrene A oxidase group CYP71AVx and the costunolide synthase group CYP71BLx.
709 However, both groups are from the related species within the Asteraceae family thus cannot be used
710 in general for functional identification. Only bootstrap values higher than 50 are shown in the tree.

711

712 **Figure 3.** GC-MS analysis of hexane extracts from *N. benthamiana* expressing in **A** *At*tHMGR and
713 *Tg*TPS2 with a GC-MS injection port temperature of 160°C (red) and of 250°C (black), in **B**
714 *At*tHMGR alone (black), *At*tHMGR and *Tg*TPS2 (red), *At*tHMGR, *Tg*TPS2 and *Tg*CYPAE2 (blue)
715 with a GC-MS injection port temperature of 250°C. * Denotes epikunzeaol thermal rearrangement
716 products. **C:** Mass spectra the elemanolides **2** and **3**.

717

718 **Figure 4**: **A**:Extracted Ion Chromatograms of epikunzeaol (**1**) [epikunzeaol disaccharide+Na]$^+$ *m/z*
719 569.74 (red) and epidihydrocostunolide [2M+Na]$^+$ *m/z* 491.32 (blue) of the LC-MS analysis of
720 methanol extract of *At*tHMGR alone, *At*tHMGR plus *Tg*TPS2, and *At*tHMGR plus *Tg*TPS2 co-
721 expressed with *Tg*CYP76AE2.
722 **B**: The MS/MS spectrum of the epikunzeaol peak at 18 minutes detected as the epikunzeaol-
723 disaccharide. The MS spectrum of epidihydrocostunolide at 27 minutes shows a *m/z* of 491.3258
724 corresponding to a sodium adduct and a dimer of *m/z* 235.1741.
725 **C**: The structure of epikunzeaol disaccharide including the fragmentation pattern.

726

727 **Figure 5**: Thermal rearrangement of **1** into the two compounds **2** and **3**. The Cope rearrangement is
728 well known for transforming germacradi-1(10),4-dienolides into elemanolides.

729

730 **Figure 6 A:** *In situ* PCR of *Tg*CYP76AE2 and *Tg*STS2 in *Thapsia garganica* L. root cross-
731 sections. All samples are stained with BM purple; blue/purple colour indicates presence of DIG

732 labelled cDNA; brown indicates the absence of the amplified cDNA target. **1-2:** negative controls
733 (*Tg*CYP76AE2) where reverse transcription (RT) was omitted. **3-4:** detection of *Tg*CYP76AE2
734 mainly in epithelial cells surrounding secretory ducts within vascular cambium. **5-6:** negative
735 controls (*Tg*TPS2) where RT was omitted. **7-8:** detection of *Tg*TPS2 mainly in epithelial cells
736 surrounding secretory ducts within vascular cambium as with *Tg*CYP76AE2. **9-10:** positive control;
737 18S ribosomal RNA to show staining in all cell types. **B:** NADI staining of *Thapsia garganica* L.
738 root cross-sections **11-14:** blue indicates presence of oxygenated or lipophilic compounds (e.g.
739 terpenoids) concentrated in epithelial cells & secretory ducts. Scale bars represent 100 μm. p =
740 periderm, ph = phloem, x = xylem, ep = epithelial cells, sd = secretory ducts, vc = vascular
741 cambium, s = starch grains.
742
743 **Figure 7.** MALDI-MSI analysis of *T. garganica* taproot section. **A:** optical image of taproot section
744 with sublimed DHB matrix, **B:** distribution of thapsigargin Na adduct, $[M+Na]^+$ *m/z* 673.3186 (calc.
745 673.31945, 1.26 ppm error), **C:** distribution of thapsigargin K adduct, $[M+K]^+$ *m/z* 689.2924 (calc.
746 689. 29339, 1.43 ppm error). Images normalized to RMS and scaled to 0-60 % of maximum signal
747 intensity using FlexImaging 4.1 to enhance visualization. Results demonstrate thapsigargin to be
748 localized to concentric circles similar to the pattern of secretory ducts.
749
750 **Figure 8. A:** Proposed biosynthesis of **1**. *Tg*CYP76AE2 is suggested to catalyze three
751 hydroxylations to obtain epidihydrocostunolide. The intermediates are based on knowledge from
752 the costunolide pathway shown in **B**. **B:** The costunolide pathway. Step one is GAS (germacrene A
753 synthase (Bouwmeester et al., 2002)) followed by three consecutive hydroxylation's by GAO
754 (germacrene A oxidase, CYP71AV2-9, (Nguyen et al., 2010; Cankar et al., 2011; Ramirez et al.,
755 2013; Eljounaidi et al., 2014)). Finally, a hydroxylation of C6 by COS (costunolide synthase,
756 CYP71BL2-5, (Ikezawa et al., 2011; Liu et al., 2011; Ramirez et al., 2013; Eljounaidi et al., 2014))
757 to yield costunolide.
758
759

Parsed Citations

Abbott E, Hall D, Hamberger B, Bohlmann J (2010) Laser microdissection of conifer stem tissues: isolation and analysis of high quality RNA, terpene synthase enzyme activity and terpenoid metabolites from resin ducts and cambial zone tissue of white spruce (Picea glauca). BMC Plant Biology 10: 106

Pubmed: Author and Title
CrossRef: Author and Title
Google Scholar: Author Only Title Only Author and Title

Adio AM (2009) Germacrenes A-E and related compounds: thermal, photochemical and acid induced transannular cyclizations. Tetrahedron 65: 1533-1552

Pubmed: Author and Title
CrossRef: Author and Title
Google Scholar: Author Only Title Only Author and Title

Andersen-Ranberg J, Kongstad KT, Nielsen MT, Jensen NB, Pateraki I, Bach SS, Hamberger B, Zerbe P, Staerk D, Bohlmann J, Møller BL, Hamberger B (2016) Expanding the Landscape of Diterpene Structural Diversity through Stereochemically Controlled Combinatorial Biosynthesis. Angewandte Chemie International Edition 55: 2142-2146

Pubmed: Author and Title
CrossRef: Author and Title
Google Scholar: Author Only Title Only Author and Title

Andersen TB, Cozzi F, Simonsen HT (2015) Optimization of biochemical screening methods for volatile and unstable sesquiterpenoids using HS-SPME-GC-MS. Chromatography 2: 277-292

Pubmed: Author and Title
CrossRef: Author and Title
Google Scholar: Author Only Title Only Author and Title

Andersen TB, Lopez CQ, Manczak T, Martinez K, Simonsen HT (2015) Thapsigargin--from Thapsia L. to mipsagargin. Molecules 20: 6113-6127

Pubmed: Author and Title
CrossRef: Author and Title
Google Scholar: Author Only Title Only Author and Title

Ando M, Tajima K, Takase K (1983) Studies on the syntheses of sesquiterpene lactones. 8. Syntheses of saussurea lactone, 8-deoxymelitensin, and 11,12-dehydro-8-deoxymelitensin via a novel fragmentation reaction. Journal of Organic Chemistry 48: 1210-1216

Pubmed: Author and Title
CrossRef: Author and Title
Google Scholar: Author Only Title Only Author and Title

Andrews SP, Ball M, Wierschem F, Cleator E, Oliver S, Hogenauer K, Simic O, Antonello A, Hunger U, Smith MD, Ley SV (2007) Total synthesis of five thapsigargins: Guaianolide natural products exhibiting sub-nanomolar SERCA inhibition. Chemistry - A European Journal 13: 5688-5712

Pubmed: Author and Title
CrossRef: Author and Title
Google Scholar: Author Only Title Only Author and Title

Appendino G, Gariboldi P (1983) The structure and chemistry of hallerin, a mixture of anomeric sesquiterpenoids from Laserpitium halleri Crantz subsp. halleri. Journal of the Chemical Society, Perkin Transactions 1: Organic and Bio-Organic Chemistry (1972-1999): 2017-2026

Pubmed: Author and Title
CrossRef: Author and Title
Google Scholar: Author Only Title Only Author and Title

Athman A, Tanz SK, Conn VM, Jordans C, Mayo GM, Ng WW, Burton RA, Conn SJ, Gilliham M (2014) Protocol: a fast and simple in situ PCR method for localising gene expression in plant tissue. Plant Methods 10: 29

Pubmed: Author and Title
CrossRef: Author and Title
Google Scholar: Author Only Title Only Author and Title

Bach SS, Bassard J-É, Andersen-Ranberg J, Møldrup ME, Simonsen HT, Hamberger B (2014) High throughput testing of terpenoid biosynthesis candidate genes using transient expression in Nicotiana benthamiana. In M Rodríguez-Concepción, ed, Plant Isoprenoids Vol 1153. Springer New York, New York, USA, pp 245-255

Pubmed: Author and Title
CrossRef: Author and Title
Google Scholar: Author Only Title Only Author and Title

Ball M, Andrews SP, Wierschem F, Cleator E, Smith MD, Ley SV (2007) Total Synthesis of Thapsigargin, a Potent SERCA Pump Inhibitor. Organic Letters 9: 663-666

Pubmed: Author and Title
CrossRef: Author and Title
Google Scholar: Author Only Title Only Author and Title

Barrero AF, Oltra JE, Alvarez M, Rosales A (2002) Synthesis of (+)-8-Deoxyvernolepin and Its 11,13-Dihydroderivative. A Novel Reaction Initiated by Sulfene Elimination Leads to the 2-Oxa-cis-decalin Skeleton. Journal of Organic Chemistry 67: 5461-5469

Pubmed: Author and Title
CrossRef: Author and Title
Google Scholar: Author Only Title Only Author and Title

Bohlmann J, Meyer-Gauen G, Croteau R (1998) Plant terpenoid synthases: Molecular biology and phylogenetic analysis. Proceedings of the National Academy of Sciences of the United States of America 95: 4126-4133
Pubmed: Author and Title
CrossRef: Author and Title
Google Scholar: Author Only Title Only Author and Title

Bouwmeester HJ, Kodde J, Verstappen FWA, Altug IG, De Kraker JW, Wallaart TE (2002) Isolation and characterization of two germacrene A synthase cDNA clones from chicory. Plant Physiology 129: 134-144
Pubmed: Author and Title
CrossRef: Author and Title
Google Scholar: Author Only Title Only Author and Title

Bowes BG, Mauseth JD (2008) Plant structure - a colour guide, Ed 2nd. Manson Publishing, London, UK
Pubmed: Author and Title
CrossRef: Author and Title
Google Scholar: Author Only Title Only Author and Title

Caissard J-C, Meekijjironenroj A, Baudino S, Anstett M-C (2004) Localization of production and emission of pollinator attractant on whole leaves of Chamaerops humilis (Arecaceae). American Journal of Botany 91: 1190-1199
Pubmed: Author and Title
CrossRef: Author and Title
Google Scholar: Author Only Title Only Author and Title

Cankar K, Houwelingen Av, Bosch D, Sonke T, Bouwmeester H, Beekwilder J (2011) A chicory cytochrome P450 mono-oxygenase CYP71AV8 for the oxidation of (+)-valencene. FEBS Letters 585: 178-182
Pubmed: Author and Title
CrossRef: Author and Title
Google Scholar: Author Only Title Only Author and Title

Cankar K, Jongedijk E, Klompmaker M, Majdic T, Mumm R, Bouwmeester H, Bosch D, Beekwilder J (2015) (+)-Valencene production in Nicotiana benthamiana is increased by down-regulation of competing pathways. Biotechnology Journal 10: 180-189
Pubmed: Author and Title
CrossRef: Author and Title
Google Scholar: Author Only Title Only Author and Title

Celedon JM, Chiang A, Yuen MMS, Diaz-Chavez ML, Madilao LL, Finnegan PM, Barbour EL, Bohlmann J (2016) Heartwood-specific transcriptome and metabolite signatures of tropical sandalwood (Santalum album) reveal the final step of (Z)-santalol fragrance biosynthesis. The Plant Journal 86: 289-299
Pubmed: Author and Title
CrossRef: Author and Title
Google Scholar: Author Only Title Only Author and Title

Chadwick M, Trewin H, Gawthrop F, Wagstaff C (2013) Sesquiterpenoids Lactones: Benefits to Plants and People. International Journal of Molecular Sciences 14: 12780
Pubmed: Author and Title
CrossRef: Author and Title
Google Scholar: Author Only Title Only Author and Title

Christensen SB, Andersen A, Smitt UW (1997) Sesquiterpenoids from Thapsia species and medicinal chemistry of the thapsigargins. Fortschritte der Chemie organischer Naturstoffe. Progress in the chemistry of organic natural products. 71: 129-167
Pubmed: Author and Title
CrossRef: Author and Title
Google Scholar: Author Only Title Only Author and Title

Christensen SB, Norup E, Rasmussen U, Madsen JØ (1984) Structure of histamine releasing guaianolides from Thapsia species. Phytochemistry 23: 1659-1663
Pubmed: Author and Title
CrossRef: Author and Title
Google Scholar: Author Only Title Only Author and Title

Chu H, Smith JM, Felding J, Baran PS (2016) Scalable Synthesis of (-)-Thapsigargin. ACS Central Science
Pubmed: Author and Title
CrossRef: Author and Title
Google Scholar: Author Only Title Only Author and Title

Collu G, Unver N, Peltenburg-Looman AM, van der Heijden R, Verpoorte R, Memelink J (2001) Geraniol 10-hydroxylase, a cytochrome P450 enzyme involved in terpenoid indole alkaloid biosynthesis. FEBS Letters 508: 215-220
Pubmed: Author and Title
CrossRef: Author and Title
Google Scholar: Author Only Title Only Author and Title

Corsi G, Pagni AM, Innocenti G (1988) Carum appuanum (Viv.) Grande (Umbelliferae). I. Histochemical and Anatomical Study. International Journal of Crude Drug Research 26: 129-136
Pubmed: Author and Title
CrossRef: Author and Title
Google Scholar: Author Only Title Only Author and Title

Curry EA, 3rd, Murry Dj Fau - Yoder C, Yoder C Fau - Fife K, Fife K Fau - Armstrong V, Armstrong V Fau - Nakshatri H, Nakshatri H Fau - O'Connell M, O'Connell M Fau - Sweeney CJ, Sweeney CJ (2004) Phase I dose escalation trial of feverfew with standardized doses of parthenolide in patients with cancer. Investigational New Drugs 22: 299-305

Pubmed: Author and Title
CrossRef: Author and Title
Google Scholar: Author Only Title Only Author and Title

David R, Carde J (1964) Histochimie-coloration differentielle des inclusions lipidiques et terpeniques des pseudophylles du pin maritime au moyen du reactif NADI. Comptes Rendus Hebdomadaires des Seances de L'Academie des Sciences 258: 1338-&
Pubmed: Author and Title
CrossRef: Author and Title
Google Scholar: Author Only Title Only Author and Title

de Kraker JW, Franssen MC, Dalm MC, de Groot A, Bouwmeester HJ (2001) Biosynthesis of germacrene A carboxylic acid in chicory roots. Demonstration of a cytochrome P450 (+)-germacrene a hydroxylase and NADP+-dependent sesquiterpenoid dehydrogenase(s) involved in sesquiterpene lactone biosynthesis. Plant Physiology 125: 1930-1940
Pubmed: Author and Title
CrossRef: Author and Title
Google Scholar: Author Only Title Only Author and Title

de Kraker JW, Franssen MCR, Joerink M, de Groot A, Bouwmeester HJ (2002) Biosynthesis of costunolide, dihydrocostunolide, and leucodin. Demonstration of cytochrome P450-catalyzed formation of the lactone ring present in sesquiterpene lactones of chicory. Plant Physiology 129: 257-268
Pubmed: Author and Title
CrossRef: Author and Title
Google Scholar: Author Only Title Only Author and Title

Deutschmann F (1969) Anatomische Studien uber die Exkretgange in Umbelliferenwurzeln. Beitrage zur Biologie der Pflanzen 45: 409-440
Pubmed: Author and Title
CrossRef: Author and Title
Google Scholar: Author Only Title Only Author and Title

Diaz-Chavez ML, Moniodis J, Madilao LL, Jancsik S, Keeling CI, Barbour EL, Ghisalberti EL, Plummer JA, Jones CG, Bohlmann J (2013) Biosynthesis of Sandalwood Oil: Santalum album CYP76F cytochromes P450 produce santalols and bergamotol. PloS One 8: e75053
Pubmed: Author and Title
CrossRef: Author and Title
Google Scholar: Author Only Title Only Author and Title

Doan NT, Paulsen ES, Sehgal P, Moller JV, Nissen P, Denmeade SR, Isaacs JT, Dionne CA, Christensen SB (2015) Targeting thapsigargin towards tumors. Steroids 97: 2-7
Pubmed: Author and Title
CrossRef: Author and Title
Google Scholar: Author Only Title Only Author and Title

Drew DP, Dueholm B, Weitzel C, Zhang Y, Sensen C, Simonsen HT (2013) Transcriptome Analysis of Thapsia laciniata Rouy Provides Insights into Terpenoid Biosynthesis and Diversity in Apiaceae. International Journal of Molecular Sciences 14: 9080-9098
Pubmed: Author and Title
CrossRef: Author and Title
Google Scholar: Author Only Title Only Author and Title

Drew DP, Krichau N, Reichwald K, Simonsen HT (2009) Guaianolides in Apiaceae: Perspectives on pharmacology and biosynthesis. Phytochemistry Reviews 8: 581-599
Pubmed: Author and Title
CrossRef: Author and Title
Google Scholar: Author Only Title Only Author and Title

Drew DP, Rasmussen SK, Avato P, Simonsen HT (2012) A comparison of headspace solid-phase microextraction and classic hydrodistillation for the identification of volatile constituents from Thapsia spp. provides insights into guaianolide biosynthesis in Apiaceae. Phytochemical Analysis 23: 44-51
Pubmed: Author and Title
CrossRef: Author and Title
Google Scholar: Author Only Title Only Author and Title

Dueholm B, Krieger C, Drew DP, Olry A, Kamo T, Taboureau O, Weitzel C, Bourgaud F, Hehn A, Simonsen HT (2015) Evolution of substrate recognition sites (SRSs) in cytochromes P450 from Apiaceae exemplified by the CYP71AJ subfamily. BMC Evolutionary Biology In press
Pubmed: Author and Title
CrossRef: Author and Title
Google Scholar: Author Only Title Only Author and Title

Dueholm B, Krieger C, Drew DP, Olry A, Kamo T, Taboureau O, Weitzel C, Bourgaud F, Hehn A, Simonsen HT (2015) Evolution of substrate recognition sites (SRSs) in cytochromes P450 from Apiaceae exemplified by the CYP71AJ subfamily. BMC Evolutionary Biology 15: 122
Pubmed: Author and Title
CrossRef: Author and Title
Google Scholar: Author Only Title Only Author and Title

Edgar RC (2004) MUSCLE: multiple sequence alignment with high accuracy and high throughput. Nucleic Acids Research 32: 1792-1797
Pubmed: Author and Title

CrossRef: Author and Title
Google Scholar: Author Only Title Only Author and Title

Eljounaidi K, Cankar K, Comino C, Moglia A, Hehn A, Bourgaud F, Bouwmeester H, Menin B, Lanteri S, Beekwilder J (2014) Cytochrome P450s from Cynara cardunculus L. CYP71AV9 and CYP71BL5, catalyze distinct hydroxylations in the sesquiterpene lactone biosynthetic pathway. Plant Science 223: 59-68
Pubmed: Author and Title
CrossRef: Author and Title
Google Scholar: Author Only Title Only Author and Title

Esau K (1940) Developmental anatomy of the fleshy storage organ of Daucus carota. Hilgardia 13: 175-209
Pubmed: Author and Title
CrossRef: Author and Title
Google Scholar: Author Only Title Only Author and Title

Fahn A (1988) Tansley Review No. 14 Secretory Tissues in Vascular Plants. The New Phytologist 108: 229-257
Pubmed: Author and Title
CrossRef: Author and Title
Google Scholar: Author Only Title Only Author and Title

Felsenstein J (1985) Confidence Limits on Phylogenies: An Approach Using the Bootstrap. Evolution 39: 783-791
Pubmed: Author and Title
CrossRef: Author and Title
Google Scholar: Author Only Title Only Author and Title

Fischer NH, Mabry TJ (1967) Structure of tamaulipin-B, a new germacranolide and the thermal conversion of a trans-1,2-divinylcyclohexane derivative into a cyclodeca-1,5-diene system. Chemical Communications: 1235-1236
Pubmed: Author and Title
CrossRef: Author and Title
Google Scholar: Author Only Title Only Author and Title

Garrod B, Lewis BG (1980) Probable role of oil ducts in carrot root tissue. Transactions of the British Mycological Society 75: 166-169
Pubmed: Author and Title
CrossRef: Author and Title
Google Scholar: Author Only Title Only Author and Title

Guindon S, Dufayard J-F, Lefort V, Anisimova M, Hordijk W, Gascuel O (2010) New Algorithms and Methods to Estimate Maximum-Likelihood Phylogenies: Assessing the Performance of PhyML 3.0. Systematic Biology 59: 307-321
Pubmed: Author and Title
CrossRef: Author and Title
Google Scholar: Author Only Title Only Author and Title

Guo J, Zhou YJ, Hillwig ML, Shen Y, Yang L, Wang Y, Zhang X, Liu W, Peters RJ, Chen X, Zhao ZK, Huang L (2013) CYP76AH1 catalyzes turnover of miltiradiene in tanshinones biosynthesis and enables heterologous production of ferruginol in yeasts. Proceedings of the National Academy of Sciences of the United States of America 110: 12108-12113
Pubmed: Author and Title
CrossRef: Author and Title
Google Scholar: Author Only Title Only Author and Title

Hamberger B, Bak S (2013) Plant P450s as versatile drivers for evolution of species-specific chemical diversity. Philosophical Transactions of the Royal Society B-Biological Sciences 368: 1471-2970
Pubmed: Author and Title
CrossRef: Author and Title
Google Scholar: Author Only Title Only Author and Title

Hamberger B, Ohnishi T, Hamberger B, Séguin A, Bohlmann J (2011) Evolution of diterpene metabolism: Sitka spruce CYP720B4 catalyzes multiple oxidations in resin acid biosynthesis of conifer defense against insects. Plant Physiology 157: 1677-1695
Pubmed: Author and Title
CrossRef: Author and Title
Google Scholar: Author Only Title Only Author and Title

Harwig J (1967) The use of histochemical reagents for cytochrome oxidase in plant tissues. The Botanical Review 33: 116-129
Pubmed: Author and Title
CrossRef: Author and Title
Google Scholar: Author Only Title Only Author and Title

Havis L (1939) Anatomy of the hypocotyl and roots of Daucus carota. Journal of Agricultural Reseach 58: 557-564
Pubmed: Author and Title
CrossRef: Author and Title
Google Scholar: Author Only Title Only Author and Title

Ikezawa N, Göpfert JC, Nguyen DT, Kim S-U, O'Maille PE, Spring O, Ro D-K (2011) Lettuce Costunolide Synthase (CYP71BL2) and Its Homolog (CYP71BL1) from Sunflower Catalyze Distinct Regio- and Stereoselective Hydroxylations in Sesquiterpene Lactone Metabolism. Journal of Biological Chemistry 286: 21601-21611
Pubmed: Author and Title
CrossRef: Author and Title
Google Scholar: Author Only Title Only Author and Title

Jarvis DE, Ho YS, Lightfoot DJ, Schmöckel SM, Li B, Borm TJA, Ohyanagi H, Mineta K, Michell CT, Saber N, Kharbatia NM, Rupper RR, Sharp AR, Dally N, Boughton BA, Woo YH, Gao G, Schijlen EGWM, Guo X, Momin AA, Negrão S, Al-Babili S, Gehring C,

Roessner U, Jung C, Murphy K, Arold ST, Gojobori T, Linden CGvd, van Loo EN, Jellen EN, Maughan PJ, Tester M (2017) The genome of Chenopodium quinoa. Nature 542: 307-312
Pubmed: Author and Title
CrossRef: Author and Title
Google Scholar: Author Only Title Only Author and Title

Jezler CN, Batista RS, Alves PB, Silva DdC, Costa LCdB (2013) Histochemistry, content and chemical composition of essential oil in different organs of Alpinia zerumbet. Ciência Rural 43: 1811-1816
Pubmed: Author and Title
CrossRef: Author and Title
Google Scholar: Author Only Title Only Author and Title

Korolev AV, Tomos AD, Bowtell R, Farrar JF (2000) Spatial and temporal distribution of solutes in the developing carrot taproot measured at single-cell resolution. Journal of Experimental Botany 51: 567-577
Pubmed: Author and Title
CrossRef: Author and Title
Google Scholar: Author Only Title Only Author and Title

Kromer K, Kreitschitz A, Kleinteich T, Gorb SN, Szumny A (2016) Oil Secretory System in Vegetative Organs of Three Arnica Taxa: Essential Oil Synthesis, Distribution and Accumulation. Plant and Cell Physiology 57: 1020-1037
Pubmed: Author and Title
CrossRef: Author and Title
Google Scholar: Author Only Title Only Author and Title

Lange BM (2015) The Evolution of Plant Secretory Structures and Emergence of Terpenoid Chemical Diversity. Annual Review of Plant Biology 66: 139-159
Pubmed: Author and Title
CrossRef: Author and Title
Google Scholar: Author Only Title Only Author and Title

Larbat R, Hehn A, Hans J, Schneider S, Jugdé H, Schneider B, Matern U, Bourgaud F (2009) Isolation and functional characterization of CYP71AJ4 encoding for the first P450 monooxygenase of angular furanocoumarin biosynthesis. Journal of Biological Chemistry 284: 4776-4785
Pubmed: Author and Title
CrossRef: Author and Title
Google Scholar: Author Only Title Only Author and Title

Larbat R, Kellner S, Specker S, Hehn A, Gontier E, Hans J, Bourgaud F, Matern U (2007) Molecular cloning and functional characterization of psoralen synthase, the first committed monooxygenase of furanocoumarin biosynthesis. Journal of Biological Chemistry 282: 542
Pubmed: Author and Title
CrossRef: Author and Title
Google Scholar: Author Only Title Only Author and Title

Liu Q, Majdi M, Cankar K, Goedbloed M, Charnikhova T, Verstappen FW, de Vos RC, Beekwilder J, van der Krol S, Bouwmeester HJ (2011) Reconstitution of the costunolide biosynthetic pathway in yeast and Nicotiana benthamiana. PLoS One 6: e23255
Pubmed: Author and Title
CrossRef: Author and Title
Google Scholar: Author Only Title Only Author and Title

Liu Q, Manzano D, Tanic N, Pesic M, Bankovic J, Pateraki I, Ricard L, Ferrer A, de Vos R, van de Krol S, Bouwmeester H (2014) Elucidation and in planta reconstitution of the parthenolide biosynthetic pathway. Metabolic engineering 23: 145-153
Pubmed: Author and Title
CrossRef: Author and Title
Google Scholar: Author Only Title Only Author and Title

Luo D, Callari R, Hamberger B, Wubshet SG, Nielsen MT, Andersen-Ranberg J, Hallstrom BM, Cozzi F, Heider H, Lindberg Moller B, Staerk D, Hamberger B (2016) Oxidation and cyclization of casbene in the biosynthesis of Euphorbia factors from mature seeds of Euphorbia lathyris L. Proceedings of the National Academy of Sciences of the United States of America 113: E5082-5089
Pubmed: Author and Title
CrossRef: Author and Title
Google Scholar: Author Only Title Only Author and Title

Luo P, Wang YH, Wang GD, Essenberg M, Chen XY (2001) Molecular cloning and functional identification of (+)-delta-cadinene-8-hydroxylase, a cytochrome P450 mono-oxygenase (CYP706B1) of cotton sesquiterpene biosynthesis. Plant Journal 28: 95-104
Pubmed: Author and Title
CrossRef: Author and Title
Google Scholar: Author Only Title Only Author and Title

Maggi F, Papa F, Giuliani C, Maleci Bini L, Venditti A, Bianco A, Nicoletti M, Iannarelli R, Caprioli G, Sagratini G, Cortese M, Ricciutelli M, Vittori S (2015) Essential oil chemotypification and secretory structures of the neglected vegetable Smyrnium olusatrum L. (Apiaceae) growing in central Italy. Flavour and Fragrance Journal 30: 139-159
Pubmed: Author and Title
CrossRef: Author and Title
Google Scholar: Author Only Title Only Author and Title

Mahalingam D, Wilding G, Denmeade S, Sarantopoulas J, Cosgrove D, Cetnar J, Azad N, Bruce J, Kurman M, Allgood VE, Carducci M (2016) Mipsagargin, a novel thapsigargin-based PSMA-activated prodrug: results of a first-in-man phase I clinical trial in patients with refractory, advanced or metastatic solid tumours. British Journal of Cancer 114: 986-994
Pubmed: Author and Title

CrossRef: Author and Title
Google Scholar: Author Only Title Only Author and Title

Muravnik LE, Kostina OV, Shavarda AL (2016) Glandular trichomes of Tussilago Farfara (Senecioneae, Asteraceae). Planta 244: 737-752
Pubmed: Author and Title
CrossRef: Author and Title
Google Scholar: Author Only Title Only Author and Title

Møller BL (2010) Dynamic Metabolons. Science 330: 1328-1329
Pubmed: Author and Title
CrossRef: Author and Title
Google Scholar: Author Only Title Only Author and Title

Nelson D (2009) The Cytochrome P450 Homepage. Human Genomics 4: 59 - 65
Pubmed: Author and Title
CrossRef: Author and Title
Google Scholar: Author Only Title Only Author and Title

Nguyen DT, Göpfert JC, Ikezawa N, MacNevin G, Kathiresan M, Conrad J, Spring O, Ro D-K (2010) Biochemical Conservation and Evolution of Germacrene A Oxidase in Asteraceae. Journal of Biological Chemistry 285: 16588-16598
Pubmed: Author and Title
CrossRef: Author and Title
Google Scholar: Author Only Title Only Author and Title

Nour-Eldin HH, Hansen BG, Norholm MH, Jensen JK, Halkier BA (2006) Advancing uracil-excision based cloning towards an ideal technique for cloning PCR fragments. Nucleic Acids Research 34: e122
Pubmed: Author and Title
CrossRef: Author and Title
Google Scholar: Author Only Title Only Author and Title

Olsson ME, Olofsson LM, Lindahl A-L, Lundgren A, Brodelius M, Brodelius PE (2009) Localization of enzymes of artemisinin biosynthesis to the apical cells of glandular secretory trichomes of Artemisia annua L. Phytochemistry 70: 1123-1128
Pubmed: Author and Title
CrossRef: Author and Title
Google Scholar: Author Only Title Only Author and Title

Paddon CJ, Westfall PJ, Pitera DJ, Benjamin K, Fisher K, McPhee D, Leavell MD, Tai A, Main A, Eng D, Polichuk DR, Teoh KH, Reed DW, Treynor T, Lenihan J, Fleck M, Bajad S, Dang G, Dengrove D, Diola D, Dorin G, Ellens KW, Fickes S, Galazzo J, Gaucher SP, Geistlinger T, Henry R, Hepp M, Horning T, Iqbal T, Jiang H, Kizer L, Lieu B, Melis D, Moss N, Regentin R, Secrest S, Tsuruta H, Vazquez R, Westblade LF, Xu L, Yu M, Zhang Y, Zhao L, Lievense J, Covello PS, Keasling JD, Reiling KK, Renninger NS, Newman JD (2013) High-level semi-synthetic production of the potent antimalarial artemisinin. Nature 496: 528-532
Pubmed: Author and Title
CrossRef: Author and Title
Google Scholar: Author Only Title Only Author and Title

Peyret H, Lomonossoff GP (2013) The pEAQ vector series: the easy and quick way to produce recombinant proteins in plants. Plant Molecular Biology 83: 51-58
Pubmed: Author and Title
CrossRef: Author and Title
Google Scholar: Author Only Title Only Author and Title

Pickel B, Drew DP, Manczak T, Weitzel C, Simonsen HT, Ro DK (2012) Identification and characterization of a kunzeaol synthase from Thapsia garganica: Implications for the biosynthesis of the pharmaceutical thapsigargin. Biochemical Journal 448: 261-271
Pubmed: Author and Title
CrossRef: Author and Title
Google Scholar: Author Only Title Only Author and Title

Poli F, Tirillini B, Tosi B, Sacchetti G, Bruni A (1995) Histological localization of coumarins in different organs of Smyrnium perfoliatum (Apiaceae). Phyton-Annales Rei Botanicae A 35: 209-217
Pubmed: Author and Title
CrossRef: Author and Title
Google Scholar: Author Only Title Only Author and Title

Ramirez AM, Saillard N, Yang T, Franssen MCR, Bouwmeester HJ, Jongsma MA (2013) Biosynthesis of Sesquiterpene Lactones in Pyrethrum (Tanacetum cinerariifolium). PLoS ONE 8: e65030
Pubmed: Author and Title
CrossRef: Author and Title
Google Scholar: Author Only Title Only Author and Title

Raucher S, Chi KW, Hwang KJ, Burks JE, Jr. (1986) Synthesis via sigmatropic rearrangement. 12. Total synthesis of (+)-dihydrocostunolide via tandem Cope-Claisen rearrangement. Journal of Organic Chemistry 51: 5503-5505
Pubmed: Author and Title
CrossRef: Author and Title
Google Scholar: Author Only Title Only Author and Title

Sanz JF, Castellano G, Marco JA (1990) Sesquiterpene lactones from Artemisia herba-alba. Phytochemistry 29: 541-545
Pubmed: Author and Title
CrossRef: Author and Title
Google Scholar: Author Only Title Only Author and Title

Schuphan W, Boek K (1960) Histologisch-chemische Untersuchungen in Speicherwurzeln der Möhre (Daucus carota L.) in Beziehung zu Rückständen nach Aldrin-und Dieldrin-Behandlung. Qualitas Plantarum et Materiae Vegetabiles 7: 213-228
Pubmed: Author and Title
CrossRef: Author and Title
Google Scholar: Author Only Title Only Author and Title

Senalik D, Simon PW (1986) Relationship between Oil Ducts and Volatile Terpenoid Content in Carrot Roots. American Journal of Botany 73: 60-63
Pubmed: Author and Title
CrossRef: Author and Title
Google Scholar: Author Only Title Only Author and Title

Setzer WN (2008) Ab initio analysis of the Cope rearrangement of germacrane sesquiterpenoids. Journal of Molecular Modeling 14: 335-342
Pubmed: Author and Title
CrossRef: Author and Title
Google Scholar: Author Only Title Only Author and Title

Simonsen HT, Weitzel C, Christensen SB (2013) Guaianolide sesquiterpenoids - Their pharmacology and biosynthesis. In KG Ramawat, JM Merillon, eds, Handbook of Natural Products - Phytochemistry, Botany and Metabolism of Alkaloids, Phenolics and Terpenes. Springer-Verlag, Berlin, Germany, pp 3069-3098
Pubmed: Author and Title
CrossRef: Author and Title
Google Scholar: Author Only Title Only Author and Title

Smitt UW, Jäger AK, Adsersen A, Gudiksen L (1995) Comparative studies in phytochemistry and fruit anatomy of Thapsia garganica and T. transtagana, Apiaceae (Umbelliferae). Botanical Journal of the Linnean Society 117: 281-292
Pubmed: Author and Title
CrossRef: Author and Title
Google Scholar: Author Only Title Only Author and Title

Steševic D, Božovic M, Tadic V, Rancic D, Stevanovic ZD (2016) Plant-part anatomy related composition of essential oils and phenolic compounds in Chaerophyllum coloratum, a Balkan endemic species. Flora - Morphology, Distribution, Functional Ecology of Plants 220: 37-51
Pubmed: Author and Title
CrossRef: Author and Title
Google Scholar: Author Only Title Only Author and Title

Stojicic D, Tošic S, Slavkovska V, Zlatkovic B, Budimir S, Janoševic D, Uzelac B (2016) Glandular trichomes and essential oil characteristics of in vitro propagated Micromeria pulegium (Rochel) Benth. (Lamiaceae). Planta 244: 393-404
Pubmed: Author and Title
CrossRef: Author and Title
Google Scholar: Author Only Title Only Author and Title

Takamatsu H, Hirai K-I (1968) Nadi Reaction of Myeloid Leucocytes and Vitamin K. Acta Histochemica et Cytochemica 1: 1-10
Pubmed: Author and Title
CrossRef: Author and Title
Google Scholar: Author Only Title Only Author and Title

Takase H, Sasaki K, Shinmori H, Shinohara A, Mochizuki C, Kobayashi H, Ikoma G, Saito H, Matsuo H, Suzuki S, Takata R (2015) Cytochrome P450 CYP71BE5 in grapevine (Vitis vinifera) catalyzes the formation of the spicy aroma compound (-)-rotundone. Journal of Experimental Botany 67: 787-798
Pubmed: Author and Title
CrossRef: Author and Title
Google Scholar: Author Only Title Only Author and Title

Takeda K (1974) Stereospecific Cope rearrangement of the germacrene-type sesquiterpenes. Tetrahedron 30: 1525-1534
Pubmed: Author and Title
CrossRef: Author and Title
Google Scholar: Author Only Title Only Author and Title

Teoh KH, Polichuk DR, Reed DW, Nowak G, Covello PS (2006) Artemisia annua L. (Asteraceae) trichome-specific cDNAs reveal CYP71AV1, a cytochrome P450 with a key role in the biosynthesis of the antimalarial sesquiterpene lactone artemisinin. FEBS Letters 580: 1411-1416
Pubmed: Author and Title
CrossRef: Author and Title
Google Scholar: Author Only Title Only Author and Title

Thastrup O, Cullen PJ, Drobak BK, Hanley MR, Dawson AP (1990) Thapsigargin, a tumor promoter, discharges intracellular Ca2+ stores by specific inhibition of the endoplasmic reticulum Ca2(+)-ATPase. Proceedings of the National Academy of Sciences of the United States of America 87: 2466-2470
Pubmed: Author and Title
CrossRef: Author and Title
Google Scholar: Author Only Title Only Author and Title

Tu Y (2011) The discovery of artemisinin (qinghaosu) and gifts from Chinese medicine. Nature Medicine 17: 1217-1220
Pubmed: Author and Title
CrossRef: Author and Title
Google Scholar: Author Only Title Only Author and Title

van Herpen TW, Cankar K, Nogueira M, Bosch D, Bouwmeester HJ, Beekwilder J (2010) Nicotiana benthamiana as a production platform for artemisinin precursors. PLoS One 5: e14222
Pubmed: Author and Title
CrossRef: Author and Title
Google Scholar: Author Only Title Only Author and Title

Weitzel C, Rønsted N, Spalik K, Simonsen HT (2014) Resurrecting deadly carrots: towards a revision of Thapsia (Apiaceae) based on phylogenetic analysis of nrITS sequences and chemical profiles. Botanical Journal of the Linnean Society 174: 620-636
Pubmed: Author and Title
CrossRef: Author and Title
Google Scholar: Author Only Title Only Author and Title

Weitzel C, Simonsen HT (2015) Cytochrome P450-enzymes involved in the biosynthesis of mono- and sesquiterpenes. Phytochemistry Reviews 14: 7-24
Pubmed: Author and Title
CrossRef: Author and Title
Google Scholar: Author Only Title Only Author and Title

Wiesner J, Ortmann R, Jomaa H, Schlitzer M (2003) New Antimalarial Drugs. Angewandte Chemie International Edition 42: 5274-5293
Pubmed: Author and Title
CrossRef: Author and Title
Google Scholar: Author Only Title Only Author and Title

Yang K, Monafared R, Wang H, Lundgren A, Brodelius P (2015) The activity of the artemisinic aldehyde ?11(13) reductase promoter is important for artemisinin yield in different chemotypes of Artemisia annua L. Plant Molecular Biology: 1-16
Pubmed: Author and Title
CrossRef: Author and Title
Google Scholar: Author Only Title Only Author and Title

Yu R, Wen W (2011) Artemisinin biosynthesis and its regulatory enzymes: Progress and perspective. Pharmacognosy Review 5: 189-194
Pubmed: Author and Title
CrossRef: Author and Title
Google Scholar: Author Only Title Only Author and Title

Zhan X, Han LA, Zhang Y, Chen D, Simonsen HT (2014) Metabolic engineering of the moss Physcomitrella patens to produce the sesquiterpenoids patchoulol and a/ß-santalene. Frontiers in Plant Science 5: 636
Pubmed: Author and Title
CrossRef: Author and Title
Google Scholar: Author Only Title Only Author and Title

Zulak KG, Bohlmann J (2010) Terpenoid Biosynthesis and Specialized Vascular Cells of Conifer Defense. Journal of Integrative Plant Biology 52: 86-97
Pubmed: Author and Title
CrossRef: Author and Title
Google Scholar: Author Only Title Only Author and Title